

Multiple-Input Auto-Encoder Guided Feature Selection for IoT Intrusion Detection Systems

Phai Vu Dinh, Diep N. Nguyen, Dinh Thai Hoang, Quang Uy Nguyen,
Eryk Dutkiewicz, and Son Pham Bao

Abstract—The heterogeneity of IoT devices and hence their diversity in data present both challenges and benefits for intrusion detection systems (IDSs). While IDSs benefit from the diversity and generalization of IoT data features, the data diversity (e.g., the heterogeneity and high dimensions of data) also makes it difficult to train effective machine learning models in IoT IDSs. This also leads to potentially redundant/noisy features that may decrease the accuracy of the detection engine in IDSs. To address these problems, this paper first introduces a novel neural network architecture called Multiple-Input Auto-Encoder (MIAE). MIAE consists of multiple sub-encoders that can process inputs from different sources with different characteristics. The MIAE model is trained in an unsupervised learning mode to transform the heterogeneous inputs into lower-dimensional representation, which helps classifiers distinguish between normal behaviour and different types of attacks. To distil and retain more relevant features but remove less important/redundant ones during the training process, we further design and embed a feature selection layer right after the representation layer of MIAE resulting in a new model called MIAEFS. This layer learns the importance of features in the representation vector, facilitating the selection of informative features from the representation vector. Experimental results on three popular benchmark IDS datasets, i.e., NSLKDD, UNSW-NB15, and IDS2017, show the superior performance of MIAE and MIAEFS compared to other methods, e.g., conventional classifiers, dimensionality reduction models, unsupervised representation learning methods with different input dimensions, and unsupervised feature selection models. Moreover, MIAE and MIAEFS combined with the Random Forest (RF) classifier achieve accuracy of 96.5% in detecting sophisticated attacks, e.g., Slowloris. The average running time for detecting an attack sample using RF with the representation of MIAE and MIAEFS is approximate $1.7E-6$ seconds, whilst the model size is lower than 1 MB. This clearly shows the effectiveness of our proposed model when deployed in practice.

Index Terms—IoT attack detection, dimensionality reduction, feature selection, Auto-Encoder, IDS, and Multimodal deep-learning.

I. INTRODUCTION

Phai. V. D is with the School of Electrical and Data Engineering, University of Technology Sydney (UTS), Sydney, NSW 2007, Australia (e-mail: Phai.D.Vu@student.uts.edu.au).

D. N. Nguyen, D. T. Hoang, and E. Dutkiewicz are with the School of Electrical and Data Engineering, the University of Technology Sydney, Sydney, NSW 2007, Australia (e-mail: {diep.nguyen, hoang.dinh, eryk.dutkiewicz}@uts.edu.au).

N. Q. Uy is with the Computer Science Department, Faculty of Information Technology, Le Quy Don Technical University, Hanoi, Vietnam (email: quanguyhn@lqdtu.edu.vn).

P. B. Son is with the University of Engineering and Technology, Vietnam National University, Hanoi, Vietnam (e-mail: sonpb@vnu.edu.vn).

Preliminary results of this work will be presented at the ICC 2024 IEEE International Conference on Communications, Denver, CO, USA [1].

THE explosive growth of IoT devices in recent years has improved every corner of our lives. However, it also leads to hundreds of thousands of malwares on the IoT networks [2]. Thus, developing an effective Intrusion Detection System (IDS) is essential to protect the IoT network [3], [4]. Unfortunately, developing a robust IDS for IoT systems is a challenging task. The complexity of the data harvested from IoT devices stems from their diverse origins, including network traffic, system logs, and application logs, collected across a wide array of IoT devices from different manufacturers. Therefore, the input/training data are highly dimensional and heterogeneous, i.e., numerous inputs with different dimensions. As a result, it is difficult for a specific model to learn simultaneously from such diverse data. Additionally, the deployment of a high-weight machine learning (ML) including a deep-learning (DL) model on IoT devices is not always possible due to their limited storage/memory/energy.

Amongst ML models, Auto-Encoders (AEs) can transfer the input data with higher dimensions into data of lower dimensions at the bottleneck layer by using non-linear transformation [5], [6]. Therefore, the AE model can effectively discover the latent structure of data to facilitate classifiers to distinguish the attack from the benign data. The advanced AE models including SAE [7] and FAE [8], attempt to use regularized terms to control data samples in the latent space to obtain better data representation. Other variants of AE, e.g., VAE, β -VAE, and VQ-VAE [9] can generate adversarial samples to balance between the skewed attack samples and the benign samples. However, the above AE variants cannot apply to multiple inputs with different dimensions. This is because the number of input dimensions is fixed for a specific model.

Multimodal Deep Learning (MDL) has recently been considered as a potential solution to address the problems of multiple inputs with different dimensions in IDSs [10], [11]. While MDL is effective in exploiting diverse features from various input sources to help classifiers used in IoT IDSs, the MDL models are mostly trained in a supervised manner using the label information in the training set. This limits their applications to the IoT IDSs due to the high labelling cost. To combine the benefit of the MDL in using multiple inputs and the AE variants using unsupervised learning in dimensionality reduction, the authors in [12] proposed Multi-modal Auto-Encoders (MAE). After that, the authors in [13] proposed Multi-modal Multi-task Masked Autoencoders (MultiMAE) to reduce the dimensions of masked image inputs, while multiple-input multiple-output convolutional autoencoder (MIMO-CAE) in [14] is used for the multipoint

channel charting problem in the wireless network. Both MAE and MultiMAE are designed with separated/parallel AEs to address multiple inputs. This allows diverse data representations from various input sources to benefit classifiers in IoT IDSs. However, it is difficult/time-consuming to train the MAE and MultiMAE models which have separated/parallel AEs and their loss functions. Unlike the MultiMAE, MIMO-CAE is designed to add the data representation of each AE at the output of the sub-encoder, and its loss function is a sum of the loss functions from each AE. This improves the training of MIMO-CAE, in comparison to that of MultiMAE [13], as the sum of loss function can be incorporated into a single model instead of multiple separate models. However, the MIMO-CAE architecture/model has two weaknesses. First, the addition of sub-representation vectors from sub-encoders can degrade the characteristics of the features, instead of diversifying them as the MDL models including MAE and MultiMAE do. Second, it is time-consuming to tune the hyper-parameters of MIMO-CAE because of the trade-off among its many loss components. Additionally, the effectiveness of MIMO-CAE in extracting useful features from multiple inputs has not been fully discussed in [14].

Given the above, we first propose a novel Multi-model Deep Learning model based on AE called Multiple-Input Auto-Encoder (MIAE). The data representation of MIAE is comprised of multiple sub-representations of sub-encoders. However, the MIAE has only one decoder instead of multiple sub-decoders, and its loss function with only one component instead of a sum function of sub-loss components. In addition, the MIAE model is trained in the unsupervised learning mode to avoid the high labelling cost. Therefore, the MIAE can transfer the heterogeneous inputs into a lower-dimensional representation to facilitate classifiers to distinguish between the normal and types of attacks. However, we observe that the representation vector of MIAE may contain both important and redundant features, as it might be influenced by noise or non-relevant sub-datasets, resulting in a decrease in classifiers' accuracy using data representation of the MIAE. This thus presents a new challenge of discarding the redundant features from the representation vector of MIAE to select the intrinsic features for classifiers.

Feature selection (FS) plays an essential role in selecting the most important and discarding redundant features to enhance the accuracy of classification models. Recently, supervised FS methods have shown promising results in selecting informative features from the original data, e.g., DFS [15], TabNet [16], FSBUF [17], and ManiFeSt [18]. The unsupervised FS methods have been proposed in the literature including, filtering methods, e.g., LS [19] and SPEC [20], wrapper-based methods, e.g., MCFS [21], UDFS [22], and NDFS [23], graph-based methods, e.g., CNAFS [24], RSOGFS [25], WPANFS [26], and UAFS-BH [27], and AE-based methods, e.g., FSGAE [28], AEFS [29], and FAE [8]. However, these filtering and wrapper methods are not suitable for IoT IDSs as they often require a huge amount of memory. For example, LS and SPEC require nearly 527 GB for an array with shape (265927, 265927) on the IDS2017 dataset [30]. In addition, the wrapper-based FS methods may depend on a specific clus-

tering algorithm. On the other hand, although other methods that rely on graph theory can be potentially applied to heterogeneous inputs, they often involve highly complex networks, demanding sophisticated algorithms for analysis. Most graph-based methods that assume linearity likely cannot capture nonlinear relationships among features. In addition, these AE-based FS methods cannot handle multiple inputs with different dimensions in a single model. Moreover, applying these FSs to the original feature space in these models may increase the model complexity that low-end IoT devices cannot afford.

To distil and retain more relevant features but remove less important/redundant ones during the training process for IoT IDSs, we further design and embed a feature selection layer right after the representation layer of MIAE. This layer learns the importance of features in the representation vector, hence facilitating the selection of informative features from the representation vector. The resulting novel neural network architecture is referred to as Multiple-Input Auto-Encoder Guided Feature Selection (MIAEFS). Similar to the authors of [31], [32], we evaluate the performance of MIAE and MIAEFS on three IoT IDS datasets including NSLKDD [33], UNSW-NB15 (UNSW) [34], and IDS2017 [30]. In addition, similar to the authors of [8], [18], [24], [35], we also assess the effectiveness of MIAEFS on an image dataset, i.e., MNIST [36], to demonstrate its ability to select the most intrinsic features rather than background features. The results show the superiority of MIAE and MIAEFS over other relevant methods. Our major contributions are as follows:

- We propose a novel neural network architecture, i.e., MIAE, that is capable of effectively addressing the multiple inputs and heterogeneous data. The MIAE model is trained in an unsupervised learning manner to avoid the high labelling cost and learn a data representation to facilitate the classifiers in distinguishing the attack from the benign.
- To distil and retain more relevant features but remove less important/redundant ones during the training process, we further design and embed a feature selection layer right after the representation layer of MIAE to learn the importance of features in the representation vector. This helps in eliminating irrelevant features from the representation vector, which assists classifiers in achieving higher accuracy, low variance, and reducing overfitting.
- We perform extensive experiments to assess the effectiveness of MIAE and MIAEFS on three benchmark datasets, i.e., NSLKDD [33], UNSW-NB15 [34], and IDS2017 [30]. The experimental results show the superior performance of MIAE and MIAEFS over conventional classifiers, dimensionality reduction, unsupervised representation learning for multiple inputs with different dimensions, and unsupervised feature selection models, in facilitating IoT IDSs. MIAE and MIAEFS combined with RF classifier achieve 96.5% in accuracy in detecting sophisticated attacks, e.g., Slowloris. The average running time for detecting an attack sample obtained by MIAE and MIAEFS combined with the RF classifier is approximately $1.7E-6$ seconds, whilst the model size is lower

TABLE I: Acronyms used in the paper.

Acronyms	Definition	Acronyms	Definition
IDSs	Intrusion detection systems	MIMO-CAE	Multiple-input Multiple-output Convolutional Autoencoder
ML	Machine Learning	MIAE	Multiple-Input Auto-Encoder
DL	Deep-learning	FS	Feature selection
DR	Dimensionality Reduction	DFS	Dynamic Feature Selection
RL	Representation Learning	PCA	Principal Component Analysis
AEs	Auto-Encoders	ICA	Independent Component Analysis
SAE	Sparse Auto-Encoders	IPCA	Incremental Principal Component Analysis
VAE	Variational Auto-Encoders	UMAP	Uniform Manifold Approximation and Projection
LR	Logistic Regression	VQ-VAE	Vector Quantized-Variational Auto-Encoders
SVM	Support Vector Machine	FAE	Fractal Auto-Encoder
DT	Decision Trees	LS	Laplacian Score
RF	Random Forests	SPEC	Spectral Feature Selection
MDL	Multimodal Deep Learning	MCFS	Multi-Cluster Feature Selection
MAE	Multi-modal Auto-Encoders	UDFS	Unsupervised Discriminative Feature Selection
MultiMAE	Multi-modal Multi-task Masked Autoencoders	FSGAE	Feature Selection Guided Auto-Encoder
AEFS	Auto-Encoder Feature Selection	MIAEFS	Multiple-input Auto-Encoder Guided Feature Selection

than 1 MB.

- We analyze data representation characteristics of MIAE and MIAEFS through simulation and quantitative analysis. We use three scores, e.g., between-class variance (d_{bet}), within-class variance (d_{wit}), and data quality (*data-quality*) [37], to measure the quality of data representation. Particularly, we test MIAEFS on an image dataset, i.e., MNIST, to showcase its capability to select the most significant and intrinsic features rather than background features.

The remainder of the paper is organised as follows. We discuss related work in Section II, and the proposed methods are presented in Section III. Next, the results of MIAE and MIAEFS are discussed in Section V. Finally, Section VI concludes and suggests the future work.

II. RELATED WORK

We provide a brief overview of unsupervised learning models used for dimensionality reduction (DR) and representation learning (RL). Additionally, we investigate models that address the challenge of handling heterogeneous data from multiple inputs with varying dimensions using unsupervised learning. Furthermore, we discuss unsupervised feature selection (FS) methods that identify the most important and intrinsic features for input classifiers. It is worth noting that DR, RL, and FS methods are widely applied in IoT IDSs because they enable the reduction in the size of detection models by utilizing data at lower dimensions than the original input. The acronyms used in this paper are presented in Table I.

A. Dimensionality Reduction and Representation Learning

DR is a method aiming to reduce the number of features in a dataset, whilst preserving the most important features. Conventional DR methods consist of Principal Component Analysis (PCA), Independent Component Analysis (ICA), Incremental Principal Component Analysis (IPCA), and Uniform Manifold Approximation and Projection (UMAP) [38]. These four DR methods, i.e., PCA, ICA, IPCA, and UMAP, are widely used in many research areas, including IDSs, due to their convenience and effectiveness. Unlike DR, RL attempts to transform the original input into a new representation to learn meaningful data directly from the input. Amongst RL models, RL based on

AE is widely applied because it uses an unsupervised learning method without the need for label information. These models include AE [5], [6], Variational Auto-Encoder (VAE), β -VAE, Vector Quantized-Variational Auto-Encoders (VQ-VAE) [9], Sparse Auto-Encoder (SAE) [7], and Fractal Auto-Encoder (FAE) [8]. First, AE is a popular neural network model for representation learning. The AE model can effectively discover the latent structure of data to facilitate IoT IDSs. Second, the advanced AE models including SAE [7] and FAE [8], attempt to use regularized terms to control data samples in the latent space of the AE to obtain better data representation to enhance the accuracy of the IoT IDSs. Forcing the regularizer term in the loss function of the AE aims to learn a compact representation of the input and capture important features. This helps classifiers using data presentation of the AE prevent overfitting. Third, variants of the AE including VAE, β -VAE, and VQ-VAE, can generate adversarial samples to balance between the skewed attack samples and the benign samples to facilitate classifiers used in the IDSs. In addition, the VAE variants enable robust learning of disentanglement of data representation, which can learn to extract exact high-level and abstract features, resulting in improving accuracy of classifiers in IoT IDSs [39]. Although the DR methods and RL models can effectively map input data from the higher dimensions to lower dimensions, they cannot handle multiple inputs with different dimensions, as the number of input dimensions is fixed for a specific model.

Using random masking or optimized masking vectors can train models with non-independent and identically distributed (non-IID) data [40]. However, the random masking may lead to a bias in the final model because it likely discards important features of the training data. In addition, both random masking and optimized masking methods may require high training complexity, leading to not being suitable for IoT IDSs. Multimodal Deep Learning (MDL) for AEs has recently been developed to address the problem of multiple inputs with different dimensions. The authors of [12] proposed Multi-modal Auto-Encoders (MAE) to combine the benefits of MDL using multiple inputs and AE using unsupervised learning for representation learning. Following that, the authors of [13] introduced Multi-modal Multi-task Masked Autoencoders (MultiMAE) to reduce the dimensions of masked image inputs, while multiple-input multiple-output convolutional au-

toencoder (MIMO-CAE) in [14] was used for the multipoint channel charting problem in wireless networks. Both MAE and MultiMAE are designed with separate/parallel AEs to handle multiple inputs. This allows for diverse data representations from various input sources to benefit classifiers in IoT IDSs. However, training the MAE and MultiMAE models with separate/parallel AEs and their loss functions can be difficult and time-consuming. Unlike the MultiMAE, multiple-input multiple-output convolutional autoencoder (MIMO-CAE) is designed to add the data representation of each AE at the output of the sub-encoder, and its loss function is the sum of the loss functions from each AE. This improves the training of MIMO-CAE since the sum of loss functions can be incorporated into a single model instead of multiple separate models. However, the addition of sub-representation vectors from sub-encoders can degrade the characteristics of the features instead of diversifying them like the MDL models, including MAE and MultiMAE do. In addition, tuning the hyper-parameters of MIMO-CAE is time-consuming due to the trade-off among its many loss components. Additionally, the effectiveness of MIMO-CAE in extracting useful features from multiple inputs has not been fully discussed in [14]. Considering the above, we propose a novel neural network architecture, i.e., MIAE, to address the problems related to data complexity, e.g., high dimensions and heterogeneity with different dimensions. MIAE aims to facilitate classifiers used in IoT IDSs by providing data representation that supports distinguishing between normal and different types of attack data. Consequently, the MIAE model becomes a key detection engine in IoT IDSs, enhancing the accuracy of the detection engine and lowering the False Alarm Rate.

B. Feature Selection

Unlike DR and RF, feature selection (FS) is the process of selecting the most important/useful features from the original features of the dataset [41]. First, filtering methods assess the importance of features based on their statistical properties such as similarity among features. Laplacian Score (LS) is a popular filtering technique that models the local data [19]. However, LS may not take advantage of the global structure of the data. Another filtering technique called Spectral Feature Selection (SPEC) uses the structure of a graph to measure the feature relevance and similarity amongst objects [20]. The SPEC uses eigenvalues and eigenvectors of the graph Laplacian matrix to calculate selective feature subsets. However, eigenvalues may not differentiate between selective and redundant features, making it difficult to identify the most important features. In addition, both LS and SPEC require a large amount of memory usage when applied to large datasets. For example, LS and SPEC require nearly 527 GB of memory for an array with shape (265927, 265927) on the IDS2017 dataset [30]. Second, wrapper methods use the clustering algorithms to evaluate and rank feature subsets that contribute to enhancing clustering performance and identify the most important/selective features. Multi-Cluster Feature Selection (MCFS) in [21] expects the cluster structure of data before measuring the feature importance using a regression model. Like MCFS but advantage,

Unsupervised Discriminative Feature Selection (UDFS) in [22] and Nonnegative Discriminative Feature Selection (NDFS) in [23] add constraints to the regression model to differentiate between selective and redundant features. Although wrapper methods can reduce the dimensionality of the feature space by grouping highly correlated features, they come with high computational cost, and are dependent on specific clustering algorithms. Overall, both filtering and wrapper methods may face challenges when applied to large datasets with a high number of features [41].

Recently, AE-based FS has been widely applied to identify important features of the input data. AE-based FS use the weight matrix of the neural network for evaluating the importance of the features. This approach allows for training large datasets using mini-batch training [42]. One example is the Feature Selection Guided Auto-Encoder (FSGAE) introduced in [28], which combines FS and AE by separating selective and redundant features into two groups of hidden units. By separating the optimization into two tasks, measuring feature selection score and reconstructing of the input of the AE, FSGAE demonstrates superiority over competing methods. Like FSGAE, the authors in [29] proposed Auto-Encoder Feature Selection (AEFS) by using the AE model and applying $l_{(2,1)}$ regularization on the weights of the first hidden layer of the encoder of the AE. This method can be conveniently trained using a loss function consisting of reconstruction error and a regularised term. Unlike FSGAE and AEFS using sparsity norm regularizations on the AE weights to determine the feature importance, fractal autoencoders (FAE) in [8] incorporate a one-to-one scoring layer and feature selection layer. These addition aims to discover global representation features and maintain diversity to enhance the generalization of the selected features. The AEFS, FSGAE, and FAE models have shown their effectiveness in FS and can be trained on highly dimensional datasets using mini-batch training [42]. However, their model complexity may increase due to the training on the original highly dimensional feature space. Moreover, AEFS, FSGAE, and FAE are unable to trained with multiple inputs with different dimensionality in a single model. Given the above, we propose a novel neural network architecture/model, i.e., MIAEFS, to address the challenge of multiple inputs. MIAEFS performs feature selection on lower dimensions of the representation vector compared to the original feature space, allowing for reduced complexity. This reduction facilitates the use of MIAEFS in IoT IDSs, which require less memory and computational capacity.

III. METHODOLOGY

A. Background

In this subsection, we present an Auto-Encoder (AE) which is a fundamental model to develop our model in the next section. AE is one of the most popular models used for representation learning as well as dimensionality reduction. The Encoder of the AE tries to transfer input data $\mathbf{x}^{(i)}$ to the latent space $\mathbf{z}^{(i)}$ by using the function $f(\mathbf{x}^{(i)}, \phi)$ where $\phi = (\mathbf{W}^{(e)}, \mathbf{b}^{(e)})$ are weights and biases of the Encoder, respectively. Next, the function $g(\mathbf{z}^{(i)}, \theta)$ attempts to map data

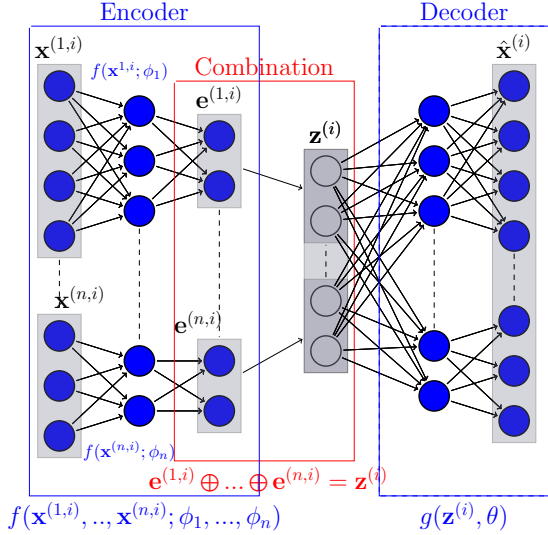


Fig. 1: Our proposed Multiple-input Auto-Encoder (MIAE) architecture.

$\mathbf{z}^{(i)}$ to the output of the Decoder $\hat{\mathbf{x}}^{(i)}$ where $\theta = (\mathbf{W}^{(d)}, \mathbf{b}^{(d)})$ are weights and biases of the Decoder, respectively. The training process of the AE model is to make the data output of the Decoder $\hat{\mathbf{x}}^{(i)}$ as close to the input data $\mathbf{x}^{(i)}$ as possible. To train the AE model, we need to minimize a reconstruction error (i.e., Mean-Square-Error (MSE)) as follows:

$$\ell_{\text{AE}}(\mathbf{X}, \phi, \theta) = \frac{1}{n} \sum_{i=1}^n \left(\mathbf{x}^{(i)} - \hat{\mathbf{x}}^{(i)} \right)^2, \quad (1)$$

where $\mathbf{X} = \{\mathbf{x}^{(1)}, \mathbf{x}^{(2)}, \dots, \mathbf{x}^{(n)}\}$ is the training dataset, and n is the number of samples. $\mathbf{x}^{(i)}$ is the i^{th} data sample of the dataset \mathbf{X} . The data sample $\mathbf{z}^{(i)}$ of the AE is considered as data representation used as the input for classifiers. Although AE is the well-known dimensionality reduction method using the unsupervised learning technique, we cannot use the AE for heterogeneous data in which the dimensionality of $\mathbf{x}^{(i)}$ and $\mathbf{x}^{(j)}$ is different, for $i, j = \{1, 2, \dots, n\}, i \neq j$. Therefore, we propose a novel neural network architecture, i.e., MIAE, to use as a dimensionality reduction technique for the heterogeneous data with different dimensions in the next section.

B. Multiple-input Auto-Encoder

In this subsection, we present the proposed deep learning neural network architecture, i.e., Multiple-input Auto-Encoder (MIAE).

1) *MIAE Architecture*: The MIAE aims to tackle the challenge as well as to leverage the benefit of the heterogeneous data problem. The architecture of MIAE is shown in Fig. 1. MIAE consists of multiple parallel encoder components to process different types of input data. Assume that the dataset \mathbf{X} includes n sub-datasets $\{\mathbf{X}^{(1)}, \mathbf{X}^{(2)}, \dots, \mathbf{X}^{(n)}\}$. Let $\mathbf{X}^{(j)} = \{\mathbf{x}^{(j,1)}, \mathbf{x}^{(j,2)}, \dots, \mathbf{x}^{(j,m)}\}$ be a sub-dataset that has its dimensionality $d^{(j)}$, and $j = \{1, 2, \dots, n\}$. $\mathbf{x}^{(j,m)}$ is a data sample of the sub-dataset $\mathbf{X}^{(j)}$. Let n and m be the number of input resources and the size of the sub-dataset $\mathbf{X}^{(j)}$, respectively. We assume that the dataset \mathbf{X} , which is heterogeneous, satisfies the following condition: $d^{(j)} \neq d^{(k)}$ if $j \neq k$, where

$j, k = \{1, 2, \dots, n\}$. $d^{(j)}$ and $d^{(k)}$ are the dimensions of two sub-datasets, i.e., $\mathbf{X}^{(j)}$ and $\mathbf{X}^{(k)}$, respectively. To simply train the MIAE model, we assume that all sub-datasets have the same number of samples, denoted as m . In scenarios where the number of samples of the sub-datasets differs, oversampling or undersampling techniques can be applied to balance these sub-datasets [43]. As observed in Fig. 1, the Encoders of the MIAE use multiple functions $f(\mathbf{x}^{(j,i)})$ of sub-encoders to transfer the multiple input data $\mathbf{x}^{(j,i)}$ into multiple latent spaces $\mathbf{e}^{(j,i)}$, as follows: $\mathbf{e}^{(j,i)} = f(\mathbf{x}^{(j,i)}, \phi_j)$, where $\phi_j = (\mathbf{W}^{(e,j)}, \mathbf{b}^{(e,j)})$ are the weights and biases of the j^{th} sub-encoder, respectively, and $i = \{1, 2, \dots, m\}, j = \{1, 2, \dots, n\}$. Next, $\mathbf{z}^{(i)}$ is defined as the latent space, and $\mathbf{z}^{(i)}$ is calculated by combining the outputs of the sub-encoders $\mathbf{e}^{(j,i)}$, as follows:

$$\mathbf{z}^{(i)} = \mathbf{e}^{(1,i)} \oplus \dots \oplus \mathbf{e}^{(n,i)}, \quad (2)$$

where \oplus denotes the combination operator. In our implementation, the combination operator is implemented by concatenating the latent vectors of different sub-encoders. For example, assume that the MIAE has two sub-encoder branches. If two vectors, i.e., $\mathbf{e}^{(1,i)} = (1, 2)$ and $\mathbf{e}^{(2,i)} = (3, 4)$, then $\mathbf{z}^{(i)} = \mathbf{e}^{(1,i)} \oplus \mathbf{e}^{(2,i)} = (1, 2, 3, 4)$. Subsequently, $\hat{\mathbf{x}}^{(i)}$ is the output of the Decoder, and it is calculated by function $g(\mathbf{z}^{(i)}, \theta)$, where $\theta = (\mathbf{W}^{(d)}, \mathbf{b}^{(d)})$ are the weights and biases of the Decoder, respectively. To satisfy the symmetry of the MIAE, the numbers of neurons in the layers of the Decoder are equal to those of the Encoder. For instance, the dimensionality of vector $\hat{\mathbf{x}}^{(i)}$ is designed as follows: $d_{\hat{\mathbf{x}}^{(i)}} = \sum_{j=1}^n d^{(j)}$, where $d^{(j)}$ is the dimensionality of the input $\mathbf{x}^{(j,i)}$.

2) *MIAE Loss Function*: MIAE aims to reproduce the multiple input data $\mathbf{x}^{(i)} = \mathbf{x}^{(1,i)} \oplus \dots \oplus \mathbf{x}^{(n,i)}$ from the output of the Decoder $\hat{\mathbf{x}}^{(i)}$. The loss function of the MIAE is calculated as follows:

$$\ell_{\text{MIAE}}(\mathbf{X}, \phi, \theta) = \frac{1}{m} \sum_{i=1}^m \left(\mathbf{x}^{(i)} - \hat{\mathbf{x}}^{(i)} \right)^2, \quad (3)$$

where $\phi = (\phi_1, \dots, \phi_n)$ is parameter sets of sub-encoders, θ is parameter sets of the Decoder, and m is the size of a sub-dataset. It is worth noting that MIAE is trained by using the unsupervised learning method, and data $\mathbf{z}^{(i)}$ is used as data representation or data of dimensionality reduction of the multiple input data $\mathbf{x}^{(i)} = \mathbf{x}^{(1,i)} \oplus \dots \oplus \mathbf{x}^{(n,i)}$. Thanks to using multiple sub-encoders, MIAE can transfer heterogeneous data from multiple input resources that have different dimensionality into lower-dimensional representation space to facilitate classifiers.

C. Multiple-input Auto-Encoder Guided Feature Selection

In this subsection, we present the proposed deep learning neural network architecture, i.e., Multiple-input Auto-Encoder guided feature selection (MIAEFS), as observed in Fig. 2. MIAEFS is an extension version of MIAE that supports the selection of robust features from the representation of $\mathbf{z}^{(i)}$.

1) *MIAEFS Architecture*: The MIAEFS has three components: an Encoder, a Feature selection, and a Decoder. Like the architecture of MIAE, MIAEFS consists of parallel encoder components to process different types of inputs which have

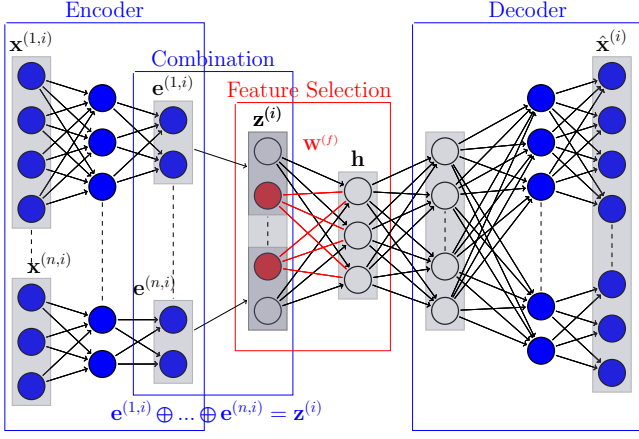


Fig. 2: Our proposed Multiple-input Auto-Encoder Guided Feature Selection (MIAEFS) architecture.

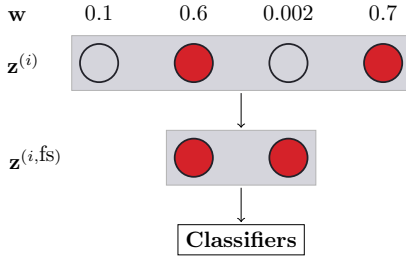


Fig. 3: Feature selection from the representation $\mathbf{z}^{(i)}$ with $\beta = 0.5$.

different dimensionality. Next, the representation data $\mathbf{z}^{(i)}$ is combined of the outputs of the sub-encoders $\mathbf{e}^{(j,i)}$, i.e., $\mathbf{e}^{(1,i)} \oplus \dots \oplus \mathbf{e}^{(n,i)} = \mathbf{z}^{(i)}$, where \oplus denotes the combination operator. Unlike the MIAE, MIAEFS has added a bottleneck layer \mathbf{h} , making the Feature Selection layer that aims to learn the importance amongst features of the representation of $\mathbf{z}^{(i)}$. Assume that $\mathbf{h}^{(i)}$ is the output of the Feature Selection layer, and it is performed by the function $f(\mathbf{z}^{(i)}, \gamma)$, where $\gamma = (\mathbf{W}^{(f)}, \mathbf{b}^{(f)})$ are the parameter sets of the Feature Selection layer. The Decoder of MIAEFS is designed to satisfy the symmetry, where the numbers of neurons in the layers of the Decoder are equal to those of the Encoder combined with the Feature Selection layer. Note that the novelty of MIAEFS is the addition of a Feature Selection layer right after the combination sub-features of sub-encoders ($\mathbf{z}^{(i)}$). This helps to decard the redundant features of $\mathbf{z}^{(i)}$, making the representation data $\mathbf{z}^{(i)}$ facilitate classifiers.

2) *MIAEFS Loss Function*: MIAEFS aims to perform two tasks. Like MIAE, the first task of MIAEFS attempts to reconstruct the multi-inputs $\mathbf{x}^{(i)} = \mathbf{x}^{(1,i)} \oplus \dots \oplus \mathbf{x}^{(n,i)}$ from the output of the Decoder $\hat{\mathbf{x}}^{(i)}$ by using the mean square error function, as follows:

$$\ell_{(\text{re})} = \frac{1}{m} \sum_{i=1}^m \left(\mathbf{x}^{(i)} - \hat{\mathbf{x}}^{(i)} \right)^2, \quad (4)$$

where m is the size of the sub-datasets. It is similar to AEFS [35], MIAEFS forces row-sparse regularization technique on the weight matrix $\mathbf{W}^{(f)}$ to rank the importance amongst

features of data representation $\mathbf{z}^{(i)}$, as follows:

$$\ell_{(\text{fs})} = \|\mathbf{W}^{(f)}\|_{2,1} = \sum_{j=1}^{d_z} \sqrt{\sum_{k=1}^{d_h} (\mathbf{W}_{j,k}^{(f)})^2}, \quad (5)$$

where d_z is the dimensionality of representation vector $\mathbf{z}^{(i)}$, and d_h is the number of neurons of the bottleneck layer $\mathbf{h}^{(i)}$. j and k are the indices of weight matrix $\mathbf{W}^{(f)}$. Therefore, the loss function of MIAEFS is as follows:

$$\ell_{\text{MIAEFS}}(\mathbf{X}, \phi, \gamma, \theta) = \frac{1}{m} \sum_{i=1}^m \left(\mathbf{x}^{(i)} - \hat{\mathbf{x}}^{(i)} \right)^2 + \alpha \|\mathbf{W}^{(f)}\|_{2,1}, \quad (6)$$

where α is a hyper-parameter to trade-off between two terms. ϕ, γ, θ are updated during training the neural network. Note that, the novelty of MIAEFS is of applying a feature selection technique on the representation vector $\mathbf{z}^{(i)}$ instead of the original input vector $\mathbf{x}^{(i)}$ like [8], [35]. This is because the representation vector $\mathbf{z}^{(i)}$ is a combination of many sub-representation vectors which may contain redundant features, leading to a decrease in the accuracy of classifiers.

3) *MIAEFS Guided Feature Selection*: After training the MIAEFS model, the weight $\mathbf{W}^{(f)}$ extracted from the Feature Selection layer is used for ranking the importance of features of the representation vector $\mathbf{z}^{(i)}$. The importance score of the j^{th} feature, i.e., $z_j^{(i)}$, is calculated as follows:

$$w_j = \sum_{k=1}^{d_h} (\mathbf{W}_{j,k}^{(f)})^2, \quad (7)$$

where d_h is the number of neurons of the bottleneck layer. $k = \{1, \dots, d_h\}$ and $j = \{1, \dots, d_z\}$ are the indices. Based on the value of vector \mathbf{w} , we rank the most important features in descending order. After that, we select top $\beta \times d_z$ most important features of the representation vector $\mathbf{z}^{(i)}$ as follows:

$$\mathbf{z}^{(i, \text{fs})} = f(\beta, \mathbf{w}, \mathbf{z}^{(i)}), \quad (8)$$

where β is the ratio of important features selected. d_z is the dimensionality of $\mathbf{z}^{(i)}$. $f(\beta, \mathbf{w}, \mathbf{z}^{(i)})$ is a function to select the number of the important features. Finally, $\mathbf{z}^{(i, \text{fs})}$ is used as the input of classifiers. For example, the dimensionality of $\mathbf{z}^{(i)}$ is 4, as observed in Fig. 3. For $\beta = 0.5$, we can select two red features as the input to classifiers.

IV. EXPERIMENTAL SETTINGS

A. Performance Metrics

1) *Detection Evaluation Metrics*: To evaluate the performance of MIAE, we use well-known classifiers, i.e., Logistic Regression (LR), Support Vector Machine (SVM), Decision Tree (DT), and Random Forests (RF) [44], to evaluate the accuracy of detection models in distinguishing the normal data from the attack data. We also use four popular metrics, e.g., *Accuracy*, *Fscore*, *Miss Detection Rate (MDR)*, and *False Alarm Rate (FAR)* [6]. First, the *Accuracy* is measured as follows:

$$\text{Accuracy} = \frac{TP + TN}{TP + TN + FP + FN}, \quad (9)$$

where *True Positive (TP)* and *False Positive (FP)* are the number of correct and incorrect predicted samples for the positive class, respectively. *True Negative (TN)* and *False Negative (FN)* are the number of correct and incorrect predicted samples for the negative classes, respectively. Second, the *Fscore* is an effective measure to evaluate imbalanced data, as calculated as follows:

$$Fscore = 2 \times \frac{Precision \times Recall}{Precision + Recall}, \quad (10)$$

where $Precision = \frac{TP}{TP+FP}$, $Recall = \frac{TP}{TP+FN}$, respectively. We also use two metrics, i.e., *MDR* and *FAR*, to evaluate the performance of attack detection models, as follows:

$$MDR = \frac{FN}{FN + TP}, \quad (11)$$

$$FAR = \frac{FP}{FP + TN}. \quad (12)$$

The detection engine in IoT IDS aims to reduce the values of *MDR* and *FAR* as small as possible.

2) *Data Quality Evaluation Metrics*: To further explain the quality of data representation from the MIAE/MIAEFS models, similar to [37], [45], we consider three measures, i.e., between-class variance (d_{bet}), within-class variance (d_{wit}), and data quality (*data-quality*). Let $\mathbf{z}^{(i,c)}$ be the i^{th} data sample of the representation of MIAE/MIAEFS, whilst n_c is the number of data samples of class label c . The mean point of the class label c is calculated as follows:

$$\mu^{(c)} = \frac{1}{n_c} \sum_{i=1}^{n_c} (\mathbf{z}^{(i,c)}). \quad (13)$$

d_{bet} is an average distance between means of different classes, as follows:

$$d_{bet} = \frac{1}{d_z \times 2} \sum_{k=1}^{d_z} \sum_{c=1}^{|C|} \sum_{c'=1}^{|C|} |\mu_k^{(c)} - \mu_k^{(c')}|^2, \quad (14)$$

where C is a set of classes, $|C|$ is the number of classes. $c, c' = \{1, 2, \dots, |C|\}$ are class labels, whilst $\mu^{(c)}, \mu^{(c')}$ are the means of classes, i.e., c and c' , respectively. d_z is the dimensionality of representation vector $\mathbf{z}^{(i,c)}$ and $k = \{1, 2, \dots, d_z\}$.

d_{wit} is the average distance between data samples of a class to its mean, as follows:

$$d_{wit} = \frac{1}{d_z \times n} \sum_{k=1}^{d_z} \sum_{c=1}^{|C|} \sum_{i=1}^{n_c} |z_k^{(i,c)} - \mu_k^{(c)}|^2, \quad (15)$$

where n is the size of the training dataset. If the value of d_{bet} is large, the means of classes are far from each other. If the value of d_{wit} is small, the data samples of a class are forced to its mean. We assume that the input data is considered as good data if data samples of a class are forced to its mean, and the means of classes are far from each other. Therefore, the representation learning models aim to make the d_{bet} as large as possible, while d_{wit} as small as possible. It is equivalent that the value of data quality is as large, as follows:

$$data-quality = \frac{d_{bet}}{d_{wit}}, \quad (16)$$

TABLE II: NSLKDD, UNSW, and IDS17 dataset information.

NSL	Classes	Normal	DoS	Probe	R2L	U2R
	No. Train	67343	45927	11656	995	52
	No. Test	9711	5741	1106	2199	37
UNSW	Classes	No. Train	No. Test	Classes	No. Train	No. Test
	Benign	37000	56000	Analysis	677	2000
	Fuzzers	6062	18184	Backdoor	583	1746
	Exploits	11132	33393	DoS	4089	12264
	Generic	18871	40000	Reconnaissance	3496	10491
	Worms	44	130	Shellcode	378	1133
IDS17	Classes	No. Train	No. Test	Classes	No. Train	No. Test
	Normal	219068	153091	DDoS	4184	2928
	DoS GoldenEye	1030	720	DoS Slowhttptest	550	385
	PortScan	15885	11120	Infiltration	4	3
	SSH-Patator	590	413	DoS Hulk	23045	16137
	DoS Slowloris	580	406	FTP-Patator	794	556
	Bot	195	138			

TABLE III: Grid search settings for typically supervised classifiers.

LR	$C=\{0.1, 0.5, 1.0, 5.0, 10.0\}$
SVM	$C=\{0.1, 0.2, 0.5, 1.0, 5.0, 10.0\}$
DT	$max_depth=\{5, 10, 20, 50, 100\}$
RF	$n_estimators=\{5, 10, 20, 50, 100, 150\}$

TABLE IV: Neural network architecture settings of MIAE.

Datasets	Branches	x^1	h_1	h_2	h_3	z	h_4	h_5	\hat{x}^t
IDS2017	$x^{1,i}$	25	20	10	5	15	30	60	80
	$x^{2,i}$	25	20	10	5				
	$x^{3,i}$	30	20	10	5				
NSLKDD	$x^{1,i}$	9	10	7	5	15	21	30	41
	$x^{2,i}$	13	10	7	5				
	$x^{3,i}$	19	10	7	5				
UNSW	$x^{1,i}$	9	10	7	5	15	21	30	42
	$x^{2,i}$	13	10	7	5				
	$x^{3,i}$	20	10	7	5				

TABLE V: Parameters of MIAEFS.

No. of branches	3,5,7,9,15, 25,35
Dimensionality of $\mathbf{z}^{(i)}$	5,10,15,20,25, 30,35,50
Ratio of features selected (β)	0.1, 0.2, 0.3, 0.4, 0.5, 0.6, 0.7, 0.8, 0.9

where $d_{wit} > 0$. It is very convenient to use three metrics, i.e., d_{bet} , d_{wit} , and *data-quality* to evaluate the data quality of the original input and representation data which have different dimensionality.

B. Datasets

In this paper, similar to the authors of [31], [32], we use three datasets often used for IoT IDSs, i.e., NSLKDD (NSL) [33], UNSW-NB15 (UNSW) [34], and IDS2017 (IDS17) [30], to perform the evaluations. First, the NSLKDD dataset in Table II has 41 features, and the dataset consists of the normal traffic and four types of attacks, e.g., DoS, R2L, Probe, and U2L. Next, we split the NSLKDD into three sub-datasets which have 9, 13, and 19 features, respectively. The first 9 features of the NSLKDD dataset relate to information extracted from the header of the packets. The next 13 features of the NSLKDD dataset relate to login information, whilst the last 19 features are statistical information. Second, the UNSW dataset is presented in Table II. The UNSW dataset includes normal data and 9 types of attacks. It is similar to the NSLKDD dataset, the UNSW dataset is split into three sub-datasets which have 9, 13, and 20 features, respectively. Third, we randomly select the numbers of features to break the

IDS2017 dataset, illustrated in Table II, into three sub-datasets which have 25, 25, and 30 features, respectively. Note that three datasets are considered extremely imbalanced, leading to lower accuracy classification of the IoT IDSs. For example, two labels, e.g., R2L and U2R are skewed labels on the NSLKDD dataset, whilst the labels named Worms, Analysis, Backdoor, and Shellcode, are the skewed labels of the UNSW dataset. In addition, we focus on the accuracy of the detection models with Slowloris attacks in the IDS2017 dataset. This is because the Slowloris attack has been mimicking the users' regular activities to lower the accuracy of the detection model. Especially, to further demonstrate the performance of MIAEFS on finding the most important/intrinsic features instead of background features, similar to the authors of [8], [18], [24], [35], we use an image dataset, i.e., MNIST [36]. There are 60000 images in the training sets and 10000 images in the testing sets. The dimensionality of each image sample is $28 \times 28 = 784$, whilst the MNIST has ten class labels corresponding to the handwritten numbers from 0 to 9.

C. Experimental Setting

To conduct experiments, we use TensorFlow and Scikit-learn frameworks [46]. Next, Min-Max normalization is used for all datasets. Similar to [47], [48] [37], we also use the grid search to tune the hyper-parameters of four classifiers, e.g., LR, SVM, DT, and RF, as shown in Table III. For all neural network models, the ADAM optimization algorithm is utilized to train the models [49]. The numbers of batch size, epoch, and learning rate are 100, 3000, and 10^{-4} , respectively. In addition, we choose the Glorot algorithm [50] to initialize the values of weights and bias, and the Tanh active function is used to implement these neural network layers. To robust performance of neural network models, the output layer of the neural network is applied to Relu active function [51], which can support surpass the “vanishing gradient problem” of Sigmoid and Tanh active functions, and “Dying ReLU” problem of the Relu active function. Next, we present the neural network architecture of MIAE in Table IV. The numbers of sub-encoders of the MIAE are equal to the numbers of sub-datasets. In addition, the number of neurons for the hidden layers of the Decoder is the sum of the neurons of the hidden layers of the sub-encoders. For example, the number of neurons of the hidden layer h_4 in the IDS2017 dataset is 30, which is equal to $10 + 10 + 10$ from three hidden layers (h_2) of three sub-encoders. For AE, VAE, β -VAE, VQ-VAE, SAE, FAE-RL, the number of neurons in the bottleneck layer is equal to $\sqrt{d_{\mathbf{x}^{(i)}}}$, where $d_{\mathbf{x}^{(i)}}$ is the dimensionality of the input $\mathbf{x}^{(i)}$ [37]. Regarding MIMOCAE and MultiMAE, the number of branches and the number of neurons of the sub-encoders are designed the same as those of MIAE. The sub-decoders of MIMOCAE and MultiMAE are symmetric to their sub-encoders. To enhance the accuracy of MIMOCAE on tabular datasets, we design a feedforward neural network instead of a convolutional neural network.

For MIAEFS, we conduct extensive experiments to show its performance on both aspects, e.g., addressing the problem of multiple inputs and the effectiveness of selecting the most

important features, to facilitate IoT IDS. First, the number of branches related to the number of inputs is tuned by a list, i.e., $\{3, 5, 7, 9, 15, 25, 35\}$, as observed in Table V. To prepare the sub-datasets corresponding to the number of branches, we separate equally by the features of the original dataset into the number of branches. For example, the training sets of the NSLDKDD have 125927 samples, and each sample has 41 features. To prepare seven sub-datasets, each sample of the first six sub-datasets has six features, and the last sub-datasets has five features ($6 + 6 + 6 + 6 + 6 + 6 + 5 = 41$). Note that, seven sub-datasets have 125927 samples which are the same as the original dataset. Next, the dimensionality of the representation vector $\mathbf{z}^{(i)}$ is a list i.e., $\{5, 10, 15, 20, 25, 30, 35, 50\}$. Depending on the dimensionality of $\mathbf{z}^{(i)}$, we can expect the maximum number of branches of MIAEFS. For example, for the 5-dimensional space of $\mathbf{z}^{(i)}$, we can test two scenarios, three branches and five branches. We also test a case in the dimensionality of $\mathbf{z}^{(i)}$ is 50 which is greater than the 41 and 42 dimensions of the original datasets, i.e., the NSLKDD and the UNSW, respectively. The ratio of the most important features selected is a list, i.e., $\{0.1, 0.2, 0.3, 0.4, 0.5, 0.6, 0.7, 0.8, 0.9\}$. The hyper-parameter α of the loss function of the MIAEFS is set to 1. Finally, the number of neurons of the bottleneck layer (\mathbf{h}) is calculated as follows: $d_{\mathbf{h}} = \sqrt{d_{\mathbf{x}^{(i)}}}$ [37]. For FAE and AEFS, the ratio of features selected is equal to that of MIAEFS. Note that, for FAE [8], the results of the RF classifier using data representation extracted from the bottleneck layer are called FAE-RL, while the results using data selected from the original input by using FS are called FAE-FS. We use FAE-RL to compare to MIAE, whilst FAE-FS is used for comparing with the MIAEFS.

V. PERFORMANCE ANALYSIS

In this section, we present the main results of MIAE and MIAEFS compared to conventional classifiers using the original input, dimensionality reduction models, and unsupervised representation learning methods for multiple inputs with different dimensions, and unsupervised feature selection models, in IoT IDSs. In addition, we also show the effectiveness of MIAE and MIAEFS in detecting sophisticated attacks, i.e., Slowloris, before discussing the complexity of the MIAE and MIAEFS models with two aspects, e.g., running time and model size. Furthermore, we extensively analyse MIAE and MIAEFS models to further explain their superior performance over other methods. Finally, we further investigate the performance of MIAEFS on finding the most intrinsic features on the image dataset, i.e., MNIST, instead of the background features.

A. Performance Evaluation of Detection Models

To evaluate the performance of data from representation learning models and feature selection models, we use four well-known classifiers, e.g., LR, SVM, DT, and RF [44]. However, due to space limitation, similar to the authors of [6], [37], we report the results of the RF classifier. In addition, we also use four metrics, i.e., *Accuracy*, *Fscore*, *FAR*, and *MDR* for all comparisons, which are used for three IoT IDS datasets including IDS2017, NSLKDD, and UNSW.

TABLE VI: Performance of MIAE compared to the other representation learning methods. RF classifier is used for evaluating the quality of representation learning models.

M	Data	AE	VAE	β -VAE	VQ-VAE	SAE	FAE-RL	MIMOC AE	MultiMAE	MIAE
Acc	IDS17	0.978	0.824	0.822	0.944	0.977	0.977	0.987	0.978	0.988
	NSL	0.842	0.501	0.504	0.843	0.839	0.856	0.840	0.864	0.883
	UNSW	0.701	0.318	0.318	0.679	0.698	0.698	0.740	0.695	0.753
Fscore	IDS17	0.974	0.744	0.743	0.937	0.973	0.975	0.985	0.973	0.986
	NSL	0.794	0.380	0.383	0.801	0.793	0.821	0.798	0.833	0.853
	UNSW	0.660	0.161	0.161	0.641	0.655	0.666	0.713	0.660	0.728
FAR	IDS17	0.079	0.824	0.822	0.176	0.088	0.070	0.058	0.082	0.054
	NSL	0.156	0.500	0.498	0.153	0.155	0.132	0.130	0.130	0.109
	UNSW	0.101	0.318	0.318	0.103	0.104	0.088	0.075	0.094	0.070
MDR	IDS17	0.022	0.176	0.178	0.056	0.023	0.020	0.013	0.022	0.012
	NSL	0.158	0.499	0.496	0.157	0.161	0.144	0.160	0.136	0.117
	UNSW	0.299	0.682	0.682	0.321	0.302	0.302	0.260	0.305	0.247

First, we compare MIAE with representation learning methods, i.e., AE and VAE variants. As observed in Table VI, the *Accuracy* and *Fscore* obtained by MIAE are significantly greater than those of AE variants and VAE variants. Moreover, the *FAR* and *MDR* obtained by MIAE are the lowest ones. In addition, the *Accuracy* obtained by MIMOC AE and MultiMAE is greater than those of AE variants. For example, MIAE achieves 0.988 in terms of the *Accuracy* on the IDS2017 dataset compared to 0.977, 0.977, 0.978, 0.987, 0.978, 0.824, 0.822, 0.944 of FAE, SAE, AE, MIMOC AE, MultiMAE, VAE, β -VAE, and VQ-AE, respectively. The *FAR* and *MDR* obtained by MIAE on IDS2017 dataset are 0.54 and 0.12, respectively. These results show the effectiveness of MIAE in processing multiple input data sources to diversify the characteristic features compared to other methods.

Second, we evaluate the results of MIAE in comparison with typical dimensionality reduction models, i.e., PCA, ICA, IPCA, and UMAP [38], as shown in Table VII. Although the results in terms of the *Accuracy* and *Fscore* of PCA, ICA, IPCA, and UMAP are approximately the same, the results of MIAE are still significantly greater than these of the four methods. For instance, the *Fscore* obtained by MIAE on the NSLKDD dataset is 0.853, whilst the results of PCA, ICA, IPCA, and UMAP are 0.831, 0.824, 0.829, and 0.804, respectively. These results show the effectiveness of MIAE in using the neural network model to learn multiple input sources to diversify the characteristic features of data compared to the traditional dimensionality reduction models.

Third, MIAE combined with the RF classifier is compared to conventional classifiers using the original data, i.e., LR, SVM, DT, and RF. The results are illustrated in Table VIII. The *Fscore* obtained by MIAE combined with RF is still greater than those of four conventional classifiers. For example, the MIAE combined with RF achieves 0.728 in terms of the *Fscore* on the UNSW dataset, while LR, SVM, DT, and RF achieve 0.614, 0.606, 0.720, and 0.727, respectively. These results show the effectiveness of MIAE in using the dimensionality reduction technique compared to the conventional classifiers using the original data.

Fourth, to evaluate the performance of data selected from the most important features of the representation vector $\mathbf{z}^{(i)}$,

TABLE VII: Performance of MIAE compared to the conventional dimensionality reduction methods. RF classifier is used for evaluating the quality of the models.

Measures	Datasets	PCA	ICA	IPCA	UMAP	MIAE
Acc	IDS17	0.973	0.975	0.973	0.970	0.988
	NSL	0.865	0.854	0.863	0.845	0.883
	UNSW	0.720	0.725	0.726	0.683	0.753
Fscore	IDS17	0.969	0.971	0.969	0.966	0.986
	NSL	0.831	0.824	0.829	0.804	0.853
	UNSW	0.684	0.692	0.696	0.649	0.728
FAR	IDS17	0.106	0.099	0.099	0.088	0.054
	NSL	0.130	0.144	0.130	0.149	0.109
	UNSW	0.086	0.084	0.084	0.094	0.070
MDR	IDS17	0.027	0.025	0.027	0.030	0.012
	NSL	0.135	0.146	0.137	0.155	0.117
	UNSW	0.280	0.275	0.274	0.317	0.247

TABLE VIII: Performance of MIAE compared to the conventional machine learning methods. The standalone (STA) methods use the original datasets instead of using representation data. The input data of the STA is combined with sub-datasets.

Measures	Datasets	STA				MIAE+RF
		LR	SVM	DT	RF	
Acc	IDS2017	0.960	0.959	0.983	0.986	0.988
	NSLKDD	0.841	0.844	0.866	0.871	0.883
	UNSW	0.673	0.672	0.743	0.757	0.753
Fscore	IDS2017	0.949	0.949	0.979	0.983	0.986
	NSLKDD	0.791	0.794	0.828	0.827	0.853
	UNSW	0.614	0.606	0.720	0.727	0.728
FAR	IDS2017	0.132	0.120	0.071	0.064	0.054
	NSLKDD	0.148	0.148	0.118	0.124	0.109
	UNSW	0.118	0.120	0.069	0.068	0.070
MDR	IDS2017	0.040	0.041	0.017	0.014	0.012
	NSLKDD	0.159	0.156	0.134	0.129	0.117
	UNSW	0.327	0.328	0.257	0.243	0.247

we compare MIAEFS with MIAE, AEFS, and FAE-FS, as observed in Table IX. Overall, the values of *Accuracy*, *Fscore*, *FAR*, and *MDR* obtained by MIAEFS are largest. For instance, MIAEFS achieves 0.990 in terms of *Accuracy* compared to 0.988, 0.986, and 0.988 of MIAE, FAE-FS, and AEFS, respectively. Interestingly, the performance of MIAE and AEFS is nearly the same. This is because MIAE can take advantage of the diversity of features from multiple inputs, whilst AEFS can find the most important features from the original feature space. These results may also explain the superior performance of MIAEFS over the three remaining methods due to the ability to combine two aspects, the diversifying features from multiple inputs like MIAE and discarding the redundant features like AEFS.

Overall, the above results show the superior performance of the MIAE and MIAEFS models over other models. The results of MIAE and MIAEFS are significantly greater than the representation learning models, e.g., AE, VAE, β -VAE, FAE, SAE, and VQ-VAE. In addition, MIAE and MIAEFS achieve the best results compared to traditional dimensionality reduction models, e.g., PCA, ICA, IPCA, and UMAP. Moreover, the results of MIAE and MIAEFS combined with the RF classifier are better than those of typical classifier models, e.g., LR, SVM, DT, and RF. The results of MIAE and MIAEFS are better than those methods using unsupervised learning for multiple inputs with different dimensions. Finally, MIAEFS reports better results in comparison with FS models, i.e., FAE-FS and AEFS. Therefore, MIAE and MIAEFS can effectively support IDSs to enhance the *Accuracy* and *Fscore* and decrease

TABLE IX: Performance of MIAEFS in comparison with feature selection methods. RF classifier is used for evaluation.

Measures	Methods	Datasets			
		IDS2017	NSLKDD	UNSW	MNIST
Acc	AEFS	0.988	0.880	0.750	0.962
	FAE-FS	0.986	0.864	0.766	0.943
	MIAE	0.988	0.883	0.753	0.965
	MIAEFS	0.990	0.891	0.769	0.970
Fscore	AEFS	0.986	0.847	0.716	0.962
	FAE-FS	0.983	0.838	0.748	0.942
	MIAE	0.986	0.853	0.728	0.965
	MIAEFS	0.988	0.867	0.751	0.970
FAR	AEFS	0.054	0.114	0.071	0.004
	FAE-FS	0.059	0.128	0.061	0.006
	MIAE	0.054	0.109	0.070	0.004
	MIAEFS	0.047	0.101	0.061	0.003
MDR	AEFS	0.012	0.120	0.250	0.038
	FAE-FS	0.014	0.136	0.234	0.058
	MIAE	0.012	0.117	0.247	0.035
	MIAEFS	0.010	0.109	0.231	0.030

TABLE X: Confusion matrix of MIAE on IDS2017 dataset.

Classes	a1	a2	a3	a4	a5	a6	a7	a8	a9	a10	a11	Acc
DoS GoldenEye (a1)	470	0	0	0	0	248	0	0	0	2	0	65.3%
PortScan (a2)	0	11120	0	0	0	0	0	0	0	0	0	100.0%
SSH-Patator (a3)	0	0	412	0	0	1	0	0	0	0	0	99.8%
DoS Slowloris (a4)	0	0	0	377	0	29	0	0	0	0	0	92.9%
Bot (a5)	0	0	0	0	125	13	0	0	0	0	0	90.6%
Normal (a6)	2	0	0	1	0	153072	0	2	0	14	0	100.0%
DdoS (a7)	0	0	0	0	0	1888	1028	0	0	12	0	35.1%
DoS Slowhttptest (a8)	0	0	0	1	0	0	0	384	0	0	0	99.7%
Infiltration (a9)	0	0	0	0	0	3	0	0	0	0	0	0.0%
DoS Hulk (a10)	9	0	0	0	0	54	1	0	0	16073	0	99.6%
FTP-Patator (a11)	0	0	0	0	0	0	0	0	0	0	556	100.0%

the *FAR* and *MDR* in detecting malicious attacks.

B. Performance Evaluation on Sophisticated Attack

This section investigates the results of MIAE and MIAEFS combined with an RF classifier in detecting sophisticated attacks, i.e., Slowloris. This is because these attacks may mimic regular user activities to evade the IDSs. Specifically, the Slowloris attacks employ a low amount of bandwidth per connection, sending requests at a low rate while using different phases of attack instead of a continuous stream [30]. Consequently, IoT IDSs relying on bandwidth may fail to detect this type of attack. This can result in higher false positives or missed detection rates in the IDSs' detection engine.

First, we present the confusion matrix result of the MIAE combined with the RF classifier on the IDS2017 dataset, as observed in Table X. MIAE combined with the RF classifier shows the high *Accuracy* in detecting the Slowloris attacks. For example, MIAE combined with RF classifier achieves 92.9%, 99.7% with two classes, e.g., **a4** (DoS Slowloris) and **a8** (DoS Slowhttptest), respectively. Therefore, the average of *Accuracy* obtained by MIAE combined with the RF classifier for the Slowloris attack on the IDS2017 dataset is 96.2%. The results show the effectiveness of MIAE combined with the RF classifier in detecting attacks using sophisticated tactics to surpass the detection engine of the IDSs.

Second, we compare of accuracy obtained by the RF classifier using data representation of MIAE and MIAEFS with two sophisticated attacks, i.e., DoS Slowloris (**a4**) and DoS Slowhttptest (**a8**), as observed in Fig. 4. Thanks to the ability to discard the redundant features from the representation vector, MIAEFS achieving accuracy on detecting **a4**

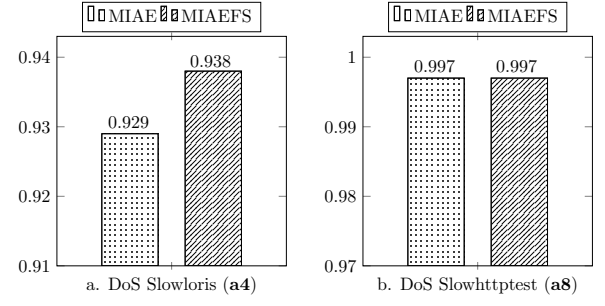


Fig. 4: Comparison accuracy of MIAE and MIAEFS TVAES in detecting sophisticated attacks.

TABLE XII: Running time and Model size of MIAE and MIAEFS combined with RF classifier.

Datasets	Running time (seconds)			Model size (KB)		
	RF	MIAE	MIAEFS	RF	MIAE	MIAEFS
IDS2017	9.7E-8	6.6E-7	1.5E-6	0.6	774	826
NSLKDD	1.5E-7	2.6E-7	1.3E-6	0.6	726	805
UNSW	1.3E-7	1.4E-7	1.9E-6	0.6	726	806

TABLE XIII: Evaluate the quality of data extracted from MIAE.

Datasets	Methods	Between-class Variance (d_{bet})	Within-class Variance (d_{wit})	Data quality
IDS2017	Original	1.970	0.027	73.0
	MIAE	1.362	0.013	104.1
NSLKDD	Original	0.618	0.038	16.4
	MIAE	0.394	0.022	18.3
UNSW	Original	0.901	0.023	38.4
	MIAE	0.721	0.022	33.0

attack is 0.938, greater than 0.929 of MIAE. For the **a8** attack, both MIAE and MIAEFS can nearly detect these attack samples of the DoS Slowhttptest attack with 0.997 in terms of accuracy. Therefore, the average accuracy obtained by MIAE and MIAEFS in detecting Slowloris attacks is 0.965. Overall, the results show that the MIAE and MIAEFS can effectively detect sophisticated attacks, i.e., Slowloris.

C. Running Time and Model Size

We investigate the running time and model size of MIAE and MIAEFS combined with the RF classifier in detecting malicious attacks. We report the results on three datasets, e.g., IDS2017, NSLKDD, and UNSW, as shown in Table XII. To conduct experiments, MIAE is set to three branches, and MIAEFS is set to five branches. The numbers of neurons in the hidden layers of MIAE and MIAEFS are $\{30 - 21 - 15 - 21 - 30\}$ and $\{35 - 30 - 25 - d_h - 25 - 30 - 35\}$, respectively. $d_h = \sqrt{d_{x^{(i)}}}$ is the number of neurons of the bottleneck layers while $d_{x^{(i)}}$ is dimensionality of the input $\mathbf{x}^{(i)}$. Overall, the average running time for detecting an attack sample obtained by MIAE and MIAEFS combined RF classifier is roundly $4.8E-7$ seconds and $1.7E-6$ seconds, respectively, whilst the model size of the MIAE combined with the RF classifier is lower than 1MB. For example, the running time obtained by MIAE and MIAEFS on the NSLKDD dataset is $2.6E-7$ seconds and $1.3E-6$ seconds, respectively, whilst the model size is 726 KB and 805 KB, respectively. The results show the effectiveness of MIAE and MIAEFS combined with the RF classifier in implementing the IoT IDSs.

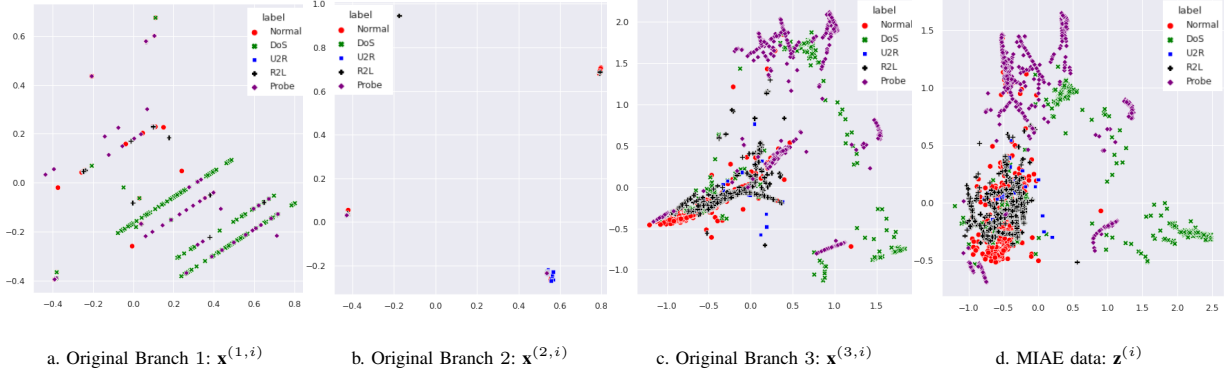


Fig. 5: Data representation of MIAE compared to original data on the NSLKDD dataset. We use PCA for mapping data into two-dimensional space.

D. Analysis of Data Representation of MIAE

We assess data extracted from the MIAE model on the NSLKDD dataset to explain why it can achieve superior performance over other methods, as shown in Fig. 5. The first three results, i.e., Figs. 5a, 5b, and 5c, are from three original sub-datasets, while the result in Fig. 5d is data extracted from the MIAE model. We use PCA to transfer data into two-dimensional space to facilitate drawing pictures. As can be seen, data samples of five classes on two figures, i.e., Figs. 5a and 5b, are overlapped, whilst the data samples of Probe attack, Normal traffic, and DoS attack, are still overlapped as shown in Fig. 5c. In contrast, the data samples of Probe attack, Normal traffic, and DoS attack can be significantly separated in Fig. 5d. The observation in Fig. 5 shows that MIAE can extract/keep/diversify the characteristic features of the data from multiple input sources. As a result, data representation from the MIAE model can facilitate classifiers in distinguishing between normal data and types of attack data.

To further explain the quality of data extracted from the MIAE model, similar to [37], we consider three measures, i.e., between-class variance (d_{bet}), within-class variance (d_{wit}), and data quality (*data-quality*). Table XIII illustrates the evaluation of data quality extracted from MIAE and the original data on three datasets, e.g., IDS2017, NSLKDD, and UNSW. As can be seen, the *data-quality* obtained by MIAE is greater than that of the original data on both IDS2017 and NSLKDD datasets. However, the *data-quality* obtained by MIAE on the UNSW dataset is lower than that of the original (33.0 vs 38.4). This can explain why the *Accuracy* obtained by MIAE combined with the RF classifier on the UNSW dataset in Table VIII is slightly lower than that of the RF classifier using the original dataset. Given the above, we can show that the MIAE models can effectively support multiple sub-datasets as well as heterogeneous data in dimensionality reduction to facilitate IDSs compared to other models.

E. Model Analysis of MIAEFS

We analyze the MIAEFS model to extensively explain its performance. First, we compare data representation obtained by applying feature selection to representation vector $\mathbf{z}^{(i)}$ and data representation at the bottleneck layer $\mathbf{h}^{(i)}$ of the MIAEFS,

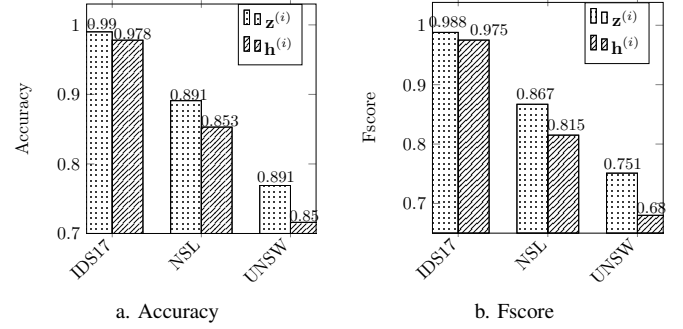


Fig. 6: Performance of MIAEFS on representation applied feature selection ($\mathbf{z}^{(i)}$) and representation at bottleneck layer ($\mathbf{h}^{(i)}$).

as observed in Fig. 6. It is clear that the accuracy and Fscore obtained by $\mathbf{z}^{(i)}$ on three datasets, i.e., IDS2017, NSL, and UNSW, are much greater than those of $\mathbf{h}^{(i)}$. For example, the accuracy obtained by representation data of $\mathbf{z}^{(i)}$ on the NSL dataset is 0.891, greater than 0.853 of the data representation of $\mathbf{h}^{(i)}$. This is because the representation of $\mathbf{z}^{(i)}$ can discard the redundant features by using a function in Equation (8), whilst the representation of $\mathbf{h}^{(i)}$ uses all features extracted from the bottleneck layer.

Second, we consider the influence of the number of important features selected on the accuracy/Fscore of the detection model, as observed in Fig. 7. In this experiment, the number of branches is set to 25, and the dimensionality of representation vector $\mathbf{z}^{(i)}$ is 50. We rank the importance of features based on Equation (7), and select the top numbers of features by using Equation (8) to obtain both training/testing sets to input the RF classifier. We can draw two interesting things. The first thing is when the number of features selected is greater than a threshold, the accuracy and Fscore obtained by the features selected are stable, and they cannot be significantly decreased. This shows that the MIAEFS can diversify features from multiple inputs to obtain such generalization features to facilitate the RF classifier. For example, the threshold of the numbers of features selected for IDS2017, NSLKDD, and UNSW, are 10, 20, 10, respectively. The second thing is that the accuracy and Fscore of the RF classifier decrease if the number of features selected are nearly the dimensionality of

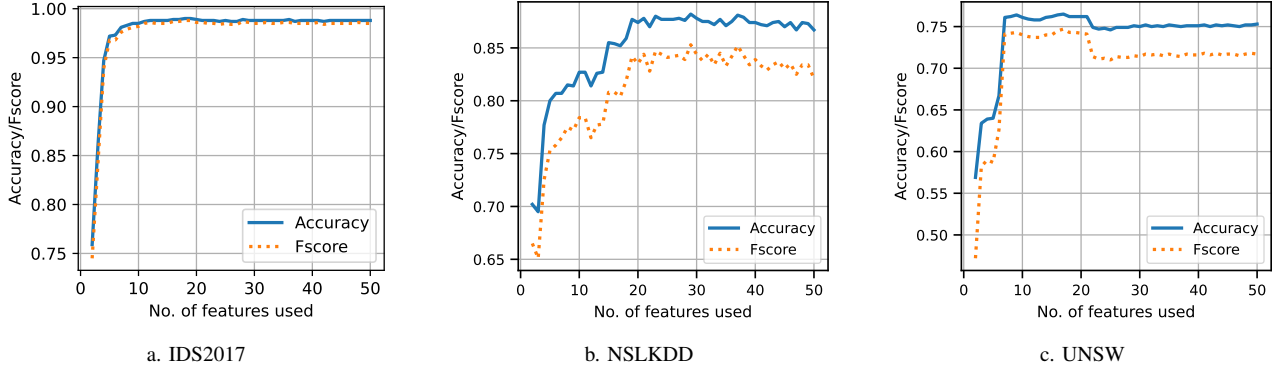


Fig. 7: Performance of MIAEFS on numbers of features used. We use 25 branches, and the dimensionality of $\mathbf{z}^{(i)}$ is 50. RF classifier is used for evaluation.

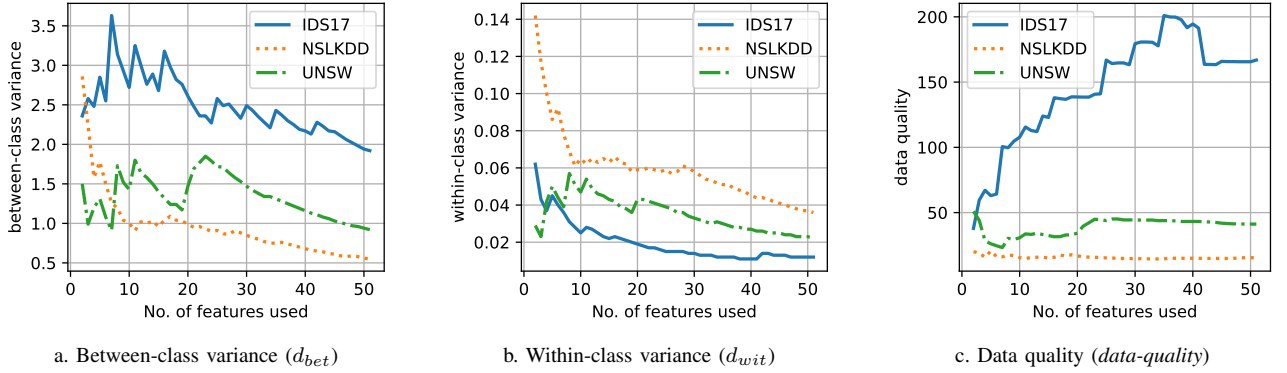


Fig. 8: Data quality of datasets created from representation $\mathbf{z}^{(i)}$ by selecting top the most important features. The dimensionality of $\mathbf{z}^{(i)}$ is 50.

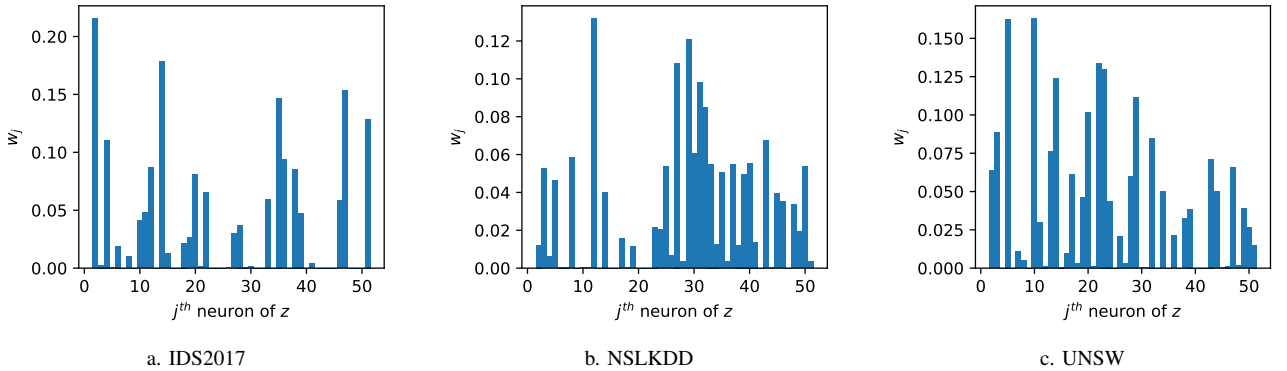


Fig. 9: The importance score of the j^{th} feature, i.e., w_j , of the representation vector $\mathbf{z}^{(i)}$. The dimensionality of $\mathbf{z}^{(i)}$ is 50. Number of branches is 25. The value of w_j is multiplied by 1000 to better illustrate.

$\mathbf{z}^{(i)}$. For instance, the accuracy and Fscore of the RF classifier obtained by using a greater 20 number of features selected from representation vector $\mathbf{z}^{(i)}$ on the UNSW dataset are lower than those by using from 10 to 20 features selected. This shows that the sub-encoders of MIAE cannot completely discard the redundant features from the multiple inputs. Therefore, MIAEFS provides a solution to select the most important features by adding the feature selection layer $\mathbf{h}^{(i)}$ right after the representation layer $\mathbf{z}^{(i)}$.

Third, we measure the quality of datasets extracted from the representation $\mathbf{z}^{(i)}$ by selecting the top important features

by using Equation (8). For example, after finishing training the MIAEFS model, we extract the testing sets from $\mathbf{z}^{(i)}$ that each data sample has 50 features. The features are ranked, and we select the top features from 1 to 50 to make new 50 datasets which have dimensionality from 1 to 50. The quality of datasets is measured by using three metrics, between-class variance (d_{bet}), within-class variance d_{wit} , and data quality (*data-quality*), as observed in Fig. 8. For the between-class variance in Fig. 8a, the values of d_{bet} increase for the first 10 features and they decrease after the 30 features are selected. It implies that the mean points of classes tend to

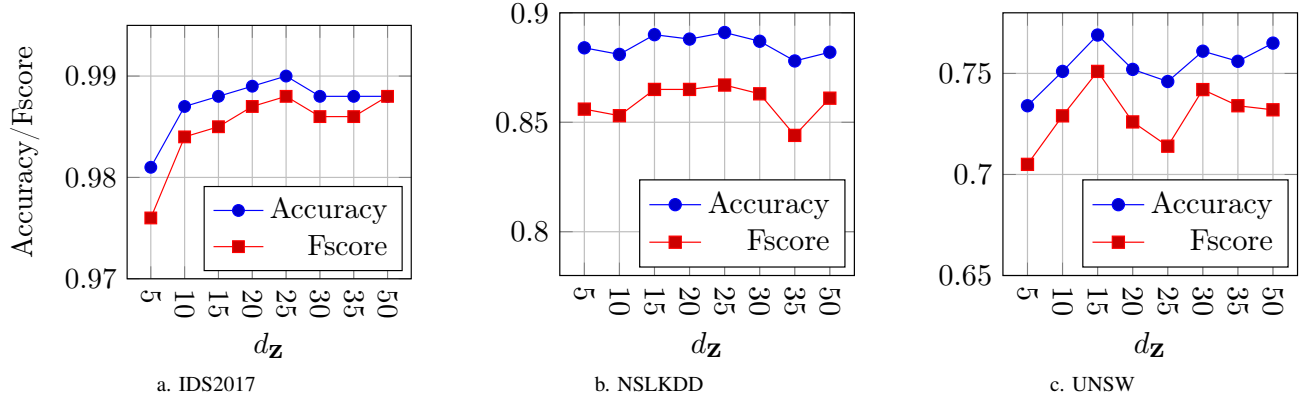


Fig. 10: Performance of MIAEFS on the numbers of dimensionality of $\mathbf{z}^{(i)}$. The number of branches is 25.

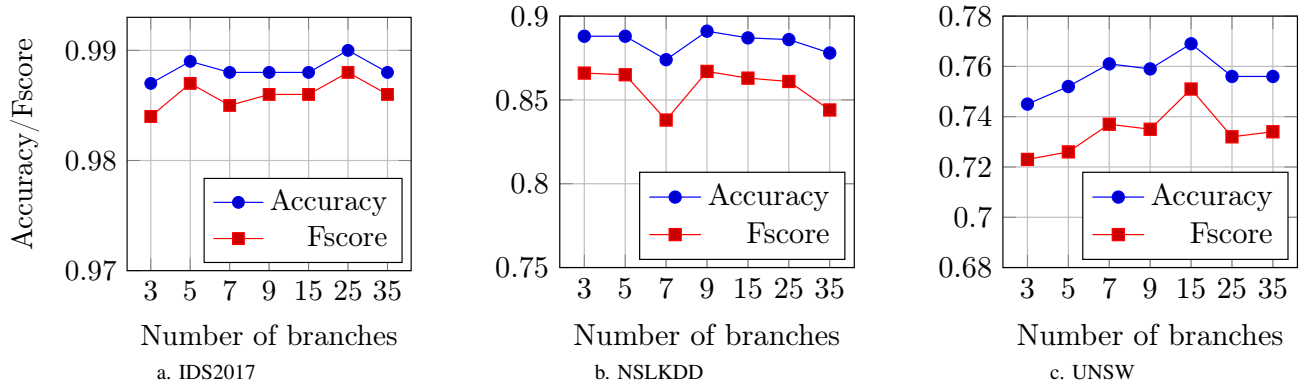


Fig. 11: Performance of MIAEFS on the numbers of branches. RF classifier is used for evaluation.

stand near when the number of features selected increases. This is because the redundant features with lower values of importance may decrease the value d_{bet} , as explained in Equation (14). Similarly, the values of d_{wit} also decrease when the number of features selected increases. This shows that the data samples of a class stand closer to each other, which contributes to making the values *data-quality* in Fig. 8c witness a growth trend for the first 30 features selected. Interestingly, the increase of the values of *data-quality* in Fig. 8c are likely the same as the values of Accuracy and Fscore in Fig. 7. This may partly explain the results presented in Fig. 7 and the effectiveness of selecting the top important features of the MIAEFS.

Fourth, we discuss the weight vector used for evaluating the importance of features of the representation vector ($\mathbf{z}^{(i)}$), as observed in Fig. 9. In this experiment, we use 25 branches for the MIAEFS, and the dimensionality of $\mathbf{z}^{(i)}$ is 50. It means that each sub-encoder provides two features in 50 features of the $\mathbf{z}^{(i)}$. Overall, the numbers of important features are spread evenly from the 1st position to the 50th position of the representation vector $\mathbf{z}^{(i)}$. This can contribute to explaining the diversity/generalization of features obtained by multiple inputs with 25 sub-datasets. Especially, there are ranges of features that have the values of w_j nearly zero. For instance, the values of \mathbf{w} from the 20th position to the 30th position, and from the

40th position to the 45th position, on the IDS2017 dataset are nearly zero. This means that these features may be ranked as redundant features and should be not selected as the input to classifiers. The experiment also shows that it is more likely beneficial to MIAE/MIAEFS to diversify features from the multiple inputs. However, there are a lot of redundant features from these multiple inputs, and they need to be discarded.

Fifth, the dimensionality of $\mathbf{z}^{(i)}$ will be discussed in Fig. 10. The accuracy and Fscore obtained by the RF classifier are low when the number of dimensions of $\mathbf{z}^{(i)}$ is too small. For example, the RF classifier using 5-dimensional data representation of $\mathbf{z}^{(i)}$ achieves 0.981 in terms of accuracy on the IDS2017 dataset compared to 0.990 when using 25-dimensional data. This is because the low-dimensional data representation may lead to losing information from the original input. Interestingly, when the dimensionality of $\mathbf{z}^{(i)}$ is greater than that of the original input, the MIAEFS still keep high values of accuracy and Fscore. For example, for the 50-dimensional space of $\mathbf{z}^{(i)}$, the accuracy of the RF classifier on the UNSW dataset is 0.765 which is slightly lower than 0.769 for 15-dimensional space (the dimensionality of the original input on the UNSW dataset is 42). For this case, the MIAEFS still keeps the diversity from multiple inputs by using multiple sub-encoders. After that, the feature selection layer can discard the redundant features. Therefore, the accuracy/Fscore of the

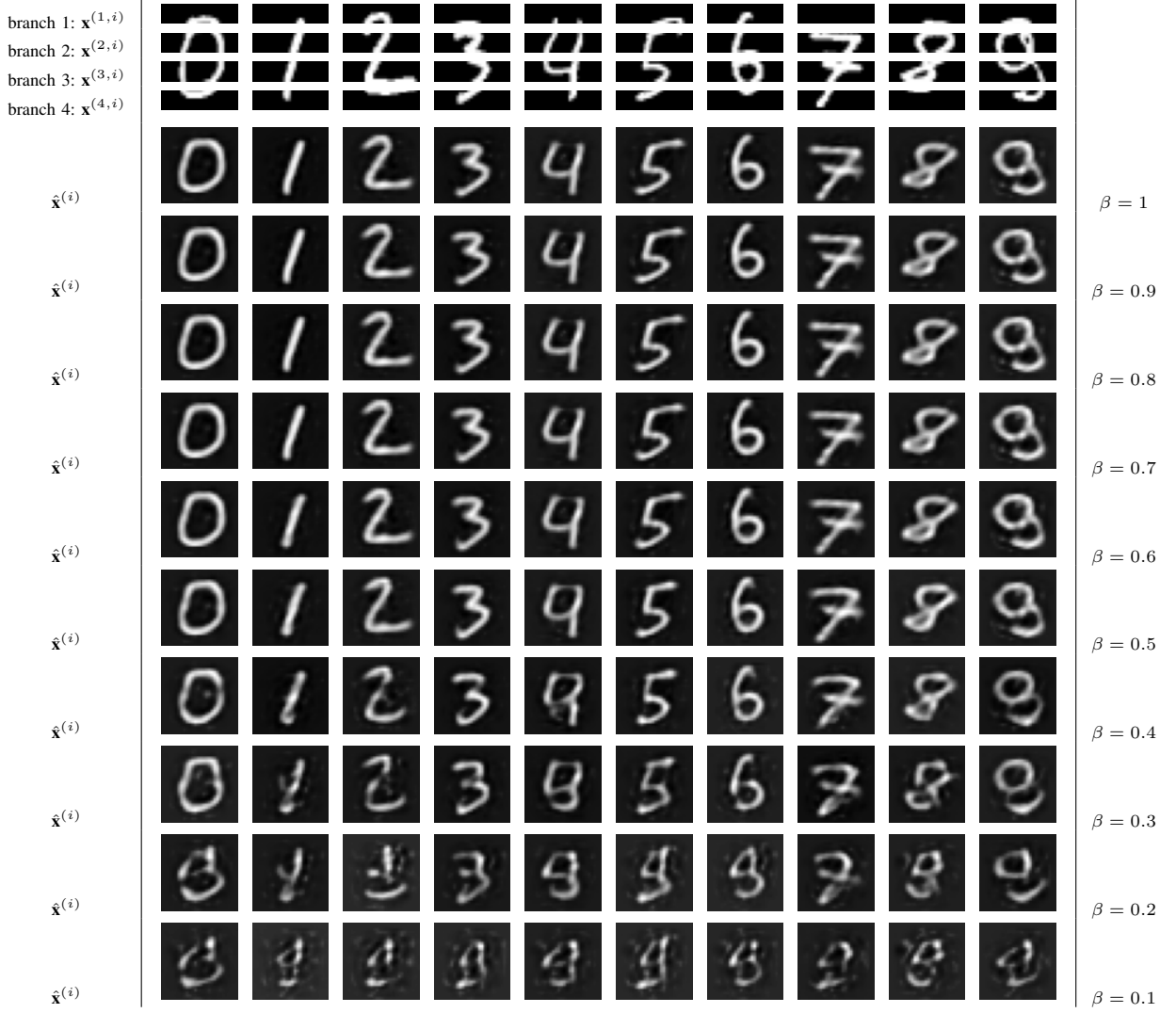


Fig. 12: Data reconstruction of MIAEFS based on the ratio of the top the most important/intrinsic feature selected. The images on the testing dataset of MNIST are used in this experiment.

RF classifier using features selected from the representation vector of MIAEFS has not been degraded.

Finally, we mention the number of branches used for MIAEFS, as observed in Fig. 11. In general, the accuracy and Fscore obtained by the RF classifier by using features selected from data representation of $\mathbf{z}^{(i)}$ are low when the number of branches is too small or too large. For example, the accuracy obtained by the RF classifier on the UNSW dataset when using three branches is 0.745, significantly lower than that of 15 and 35 branches, i.e., 0.769 and 0.756, respectively. The low number of branches may not assist the diversity of features from multiple inputs, whilst the large number of branches likely keeps the redundant features from sub-representation data of the sub-encoders of the MIAE/MIAEFS. Overall, the above results can explain the superior performance of MIAEFS over other methods. This is because MIAEFS can diversify features from multiple inputs, while its model can discard redundant features to facilitate classifiers.

F. Performance of MIAEFS on Image Dataset

In this subsection, we further discuss the performance of MIAEFS on the MNIST dataset on finding the most important/intrinsic features instead of background features. In these experiments, we illustrate the reconstructed images $\hat{\mathbf{x}}^{(i)}$ from the most important features selected from the representation vector $\mathbf{z}^{(i)}$. After training the MIAEFS model with four sub-datasets by using four branches of sub-encoders, we select the ratio of the top the most important features of $\mathbf{z}^{(i)}$ to input the Decoder to obtain the reconstructed images, as observed in Equation (8). For the redundant features, we set them to 0. For example, vector $\mathbf{z}^{(i)}$ has 4 features, i.e., $\{z_1^{(i)}, z_2^{(i)}, z_3^{(i)}, z_4^{(i)}\}$. If $z_1^{(i)}, z_3^{(i)}$ are the redundant features, we set $z_1^{(i)} = 0, z_3^{(i)} = 0$ and use vector $\{0, z_2^{(i)}, 0, z_4^{(i)}\}$ to input to the Decoder of MIAEFS. The ratio β is a list of $\{0.1, 0.2, 0.3, 0.4, 0.5, 0.6, 0.7, 0.8, 0.9, 1.0\}$. For the MNIST dataset, the number of branches is four.

Fig. 12 illustrates the images from number 0 to number 9, which are reconstructed by the ratio of the top the most important feature selected from representation vector $\mathbf{z}^{(i)}$. In

general, for $\beta \geq 0.5$, people can recognize the handwritten numbers from 0 to 9. For $\beta = 0.3$, one can detect the handwritten numbers, i.e., 0, 2, 3, 5, 6, and 8. For $\beta = 0.1$ and $\beta = 0.2$, ones find it difficult to determine the handwritten numbers. The results show that MIAEFS can select/keep the most important/intrinsic features from 4 sub-encoders, and these features stand for the intrinsic features of an image instead of the background features.

VI. CONCLUSIONS

This paper first proposed a novel deep neural network, i.e., MIAE, to address the heterogeneous data problem in IoT IDSs. MIAE was trained in an unsupervised learning manner using multiple sub-datasets with different dimensions. We extensively conducted experiments on three datasets often used for IoT IDSs, e.g., IDS2017, NSLKDD, and UNSW. The experimental results showed that MIAE combined with an RF classifier achieved the best results in comparison with conventional classifiers, dimensionality reduction models, and unsupervised representation learning methods for multiple inputs with different dimensions. MIAE combined with RF classifier also achieved 96.5% in *Accuracy* in detecting sophisticated attacks, e.g., Slowloris. We further performed experiments to explain the results obtained by MIAE. In addition, the running time and model size of MIAE were suitable for deployment on IoT devices.

However, we considered that the representation vector of MIAE had redundant features due to not completely removing from the sub-encoders of the MIAE. Therefore, to extensively address and take advantage of the data from multiple inputs, we further proposed a novel deep neural network architecture/model, i.e., MIAEFS, for both representation learning and feature selection. MIAEFS inherited the sub-encoders of MIAE to diversify features from multiple inputs, whilst the feature selection layer was right after the representation layer to learn the most important features of the representation vector. We conducted extensive experiments to show the superiority of MIAEFS over other related methods in distinguishing the normal and different types of attack samples. In addition, we intensively explain the superperformance of MIAEFS on both IoT IDS datasets and image datasets, i.e., MNIST.

In the future, one can extend our work in different directions. First, the paper applied $l_{(2,1)}$ regularization to the representation space of MIAEFS, however, one can apply $l_{(2,0)}$ regularization vector like the authors of [52]. Second, the hyper-parameter α in the loss function of the MIAEFS was determined via trial and error. It could be better to find another approach to automatically select the good value for each dataset, i.e., bayesian optimization [53]. Last but not least, the MIAE and MIAEFS models were only used for providing data representation to facilitate classifiers. Therefore, one can develop new models based on MIAE architecture to apply to anomaly detection.

REFERENCES

- [1] P. V. Dinh, D. T. Hoang, N. Q. Uy, D. N. Nguyen, S. P. Bao, and E. Dutkiewicz, "Multiple-input auto-encoder for iot intrusion detection systems with heterogeneous inputs," forthcoming in IEEE International Conference on Communications (ICC 2024), Denver, CO, USA, 2024.
- [2] B. G. Doan, S. Yang, P. Montague, O. De Vel, T. Abraham, S. Camtepe, S. S. Kanhere, E. Abbasnejad, and D. C. Ranasinghe, "Feature-space bayesian adversarial learning improved malware detector robustness," in *Proceedings of the AAAI Conference on Artificial Intelligence*, vol. 37, no. 12, 2023, pp. 14 783–14 791.
- [3] W. Hu, J. Gao, Y. Wang, O. Wu, and S. Maybank, "Online adaboost-based parameterized methods for dynamic distributed network intrusion detection," *IEEE Transactions on Cybernetics*, vol. 44, no. 1, pp. 66–82, Jan. 2013.
- [4] O. Y. Al-Jarrah, O. Alhussein, P. D. Yoo, S. Muhaidat, K. Taha, and K. Kim, "Data randomization and cluster-based partitioning for botnet intrusion detection," *IEEE Transactions on Cybernetics*, vol. 46, no. 8, pp. 1796–1806, Oct. 2015.
- [5] P. Vincent, H. Larochelle, I. Lajoie, Y. Bengio, and P.-A. Manzagol, "Stacked denoising autoencoders: Learning useful representations in a deep network with a local denoising criterion," *Journal of Machine Learning Research*, vol. 11, no. Dec, pp. 3371–3408, 2010.
- [6] N. Shone, T. N. Ngoc, V. D. Phai, and Q. Shi, "A deep learning approach to network intrusion detection," *IEEE Transactions on Emerging Topics in Computational Intelligence*, vol. 2, no. 1, pp. 41–50, Feb. 2018.
- [7] M. Al-Qatf, Y. Lasheng, M. Al-Habib, and K. Al-Sabahi, "Deep learning approach combining sparse autoencoder with svm for network intrusion detection," *IEEE Access*, vol. 6, pp. 52 843–52 856, Sept. 2018.
- [8] X. Wu and Q. Cheng, "Fractal autoencoders for feature selection," in *Proceedings of the AAAI Conference on Artificial Intelligence*, vol. 35, no. 12, Palo Alto, California USA, 2021, pp. 10 370–10 378.
- [9] Y. Yang, K. Zheng, B. Wu, Y. Yang, and X. Wang, "Network intrusion detection based on supervised adversarial variational auto-encoder with regularization," *IEEE Access*, vol. 8, pp. 42 169–42 184, Feb. 2020.
- [10] T. Kim, B. Kang, M. Rho, S. Sezer, and E. G. Im, "A multimodal deep learning method for android malware detection using various features," *IEEE Transactions on Information Forensics and Security*, vol. 14, no. 3, pp. 773–788, Mar. 2018.
- [11] G. Aceto, D. Ciunzo, A. Montieri, and A. Pescapè, "Mimetic: Mobile encrypted traffic classification using multimodal deep learning," *Computer Networks*, vol. 165, p. 106944, Dec. 2019.
- [12] J. Ngiam, A. Khosla, M. Kim, J. Nam, H. Lee, and A. Y. Ng, "Multimodal deep learning," in *Proceedings of the 28th International Conference on Machine Learning (ICML-11)*, Bellevue, Washington, USA, 2011, pp. 689–696.
- [13] R. Bachmann, D. Mizrahi, A. Atanov, and A. Zamir, "Multimae: Multimodal multi-task masked autoencoders," in *Computer Vision—ECCV 2022: 17th European Conference, Tel Aviv, Israel, October 23–27, 2022, Proceedings, Part XXXVII*, Tel Aviv, Israel, 2022, pp. 348–367.
- [14] C. Geng, H. Huang, and J. Langerman, "Multipoint channel charting with multiple-input multiple-output convolutional autoencoder," in *2020 IEEE/ION Position, Location and Navigation Symposium (PLANS)*, Portland, OR, USA, 2020, pp. 1022–1028.
- [15] I. C. Covert, W. Qiu, M. Lu, N. Y. Kim, N. J. White, and S.-I. Lee, "Learning to maximize mutual information for dynamic feature selection," in *International Conference on Machine Learning*, Honolulu, Hawaii USA, 2023, pp. 6424–6447.
- [16] S. O. Arik and T. Pfister, "Tabnet: Attentive interpretable tabular learning," in *Proceedings of the AAAI Conference on Artificial Intelligence*, vol. 35, held virtually, May 2021, pp. 6679–6687.
- [17] W. Zheng, S. Chen, Z. Fu, F. Zhu, H. Yan, and J. Yang, "Feature selection boosted by unselected features," *IEEE Transactions on Neural Networks and Learning Systems*, vol. 33, no. 9, pp. 4562–4574, Mar. 2021.
- [18] D. Cohen, T. Shnitzer, Y. Kluger, and R. Talmon, "Few-sample feature selection via feature manifold learning," in *Proceedings of the 40th International Conference on Machine Learning*, ser. Proceedings of Machine Learning Research, vol. 202, Hawaii Convention Center, 2023, pp. 6296–6319.
- [19] X. He, D. Cai, and P. Niyogi, "Laplacian score for feature selection," in *Advances in Neural Information Processing Systems 18 (NIPS 2005)*, Vancouver, British Columbia, Canada, 2005, p. 507–514.
- [20] Z. Zhao and H. Liu, "Spectral feature selection for supervised and unsupervised learning," in *Proceedings of the 24th International Conference on Machine learning*, Corvallis, Oregon, United States, 2007, pp. 1151–1157.
- [21] D. Cai, C. Zhang, and X. He, "Unsupervised feature selection for multi-cluster data," in *Proceedings of the 16th ACM SIGKDD International Conference on Knowledge Discovery and Data Mining*, Washington, District of Columbia, United States, 2010, pp. 333–342.
- [22] Y. Yang, H. T. Shen, Z. Ma, Z. Huang, and X. Zhou, " $l_{2,1}$ -norm regularized discriminative feature selection for unsupervised learning," in *IJCAI*

- International Joint Conference on Artificial Intelligence*, Barcelona, Catalonia, Spain, 2011, pp. 1589 – 1594.
- [23] Z. Li, Y. Yang, J. Liu, X. Zhou, and H. Lu, “Unsupervised feature selection using nonnegative spectral analysis,” in *Proceedings of the AAAI Conference on Artificial Intelligence*, vol. 26, no. 1, Toronto, Ontario, Canada, 2012, pp. 1026–1032.
- [24] A. Yuan, M. You, D. He, and X. Li, “Convex non-negative matrix factorization with adaptive graph for unsupervised feature selection,” *IEEE Transactions on Cybernetics*, vol. 52, no. 6, pp. 5522–5534, Jun. 2020.
- [25] F. Nie, X. Dong, L. Tian, R. Wang, and X. Li, “Unsupervised feature selection with constrained $l_{2,0}$ -norm and optimized graph,” *IEEE Transactions on Neural Networks and Learning Systems*, vol. 33, no. 4, pp. 1702–1713, 2020.
- [26] Z. Li, F. Nie, D. Wu, Z. Hu, and X. Li, “Unsupervised feature selection with weighted and projected adaptive neighbors,” *IEEE Transactions on Cybernetics*, vol. 53, no. 2, Feb. 2023.
- [27] D. Shi, L. Zhu, J. Li, Z. Zhang, and X. Chang, “Unsupervised adaptive feature selection with binary hashing,” *IEEE Transactions on Image Processing*, vol. 32, pp. 838–853, Jan. 2023.
- [28] S. Wang, Z. Ding, and Y. Fu, “Feature selection guided auto-encoder,” in *Proceedings of the AAAI Conference on Artificial Intelligence*, vol. 31, no. 1, San Francisco, California USA, 2017, pp. 2725–2731.
- [29] K. Han, Y. Wang, C. Zhang, C. Li, and C. Xu, “Autoencoder inspired unsupervised feature selection,” in *2018 IEEE International Conference on Acoustics, Speech and Signal Processing (ICASSP)*, Calgary, Alberta, Canada, 2018, pp. 2941–2945.
- [30] I. Sharafaldin, A. Ghabibi Lashkari, and A. Ghorbani, “Toward generating a new intrusion detection dataset and intrusion traffic characterization,” Jan. 2018, pp. 108–116.
- [31] A. Thakkar and R. Lohiya, “Attack classification of imbalanced intrusion data for iot network using ensemble-learning-based deep neural network,” *IEEE Internet of Things Journal*, vol. 10, no. 13, pp. 11 888–11 895, Feb. 2023.
- [32] A. Alhowaide, I. Alsmadi, and J. Tang, “Ensemble detection model for iot ids,” *Internet of Things*, vol. 16, p. 100435, Dec. 2021.
- [33] M. Tavallaei, E. Bagheri, W. Lu, and A. A. Ghorbani, “A detailed analysis of the kdd cup 99 data set,” in *2009 IEEE Symposium on Computational Intelligence for Security and Defense Applications*, Ottawa, ON, Canada, 2009, pp. 1–6.
- [34] N. Moustafa and J. Slay, “Unsw-nb15: a comprehensive data set for network intrusion detection systems (unsw-nb15 network data set),” in *2015 Military Communications and Information Systems Conference (MILCIS)*, 2015, pp. 1–6.
- [35] K. Han, Y. Wang, C. Zhang, C. Li, and C. Xu, “Autoencoder inspired unsupervised feature selection,” in *2018 IEEE International Conference on Acoustics, Speech and Signal Processing (ICASSP)*, Seoul, Korea, 2018, pp. 2941–2945.
- [36] L. Deng, “The mnist database of handwritten digit images for machine learning research,” *IEEE Signal Processing Magazine*, vol. 29, no. 6, pp. 141–142, Oct. 2012.
- [37] P. V. Dinh, Q. U. Nguyen, D. T. Hoang, D. N. Nguyen, S. P. Bao, and E. Dutkiewicz, “Constrained twin variational auto-encoder for intrusion detection in iot systems,” *IEEE Internet of Things Journal*, pp. 1–14, 2023.
- [38] Á. Huertas-García, A. Martín, J. Huertas-Tato, and D. Camacho, “Exploring dimensionality reduction techniques in multilingual transformers,” *Cognitive Computation*, vol. 15, no. 2, pp. 590–612, Oct. 2023.
- [39] C. Qiu, Y. Geng, J. Lu, K. Chen, S. Zhu, Y. Su, G. Nan, C. Zhang, J. Fu, Q. Cui *et al.*, “3d-ids: Doubly disentangled dynamic intrusion detection,” in *Proceedings of the 29th ACM SIGKDD Conference on Knowledge Discovery and Data Mining*, Long Beach, CA, USA, 2023, pp. 1965–1977.
- [40] M. Setayesh, X. Li, and V. W. Wong, “Perfedmask: Personalized federated learning with optimized masking vectors,” in *The Eleventh International Conference on Learning Representations*, 2023.
- [41] S. Solorio-Fernández, J. A. Carrasco-Ochoa, and J. F. Martínez-Trinidad, “A review of unsupervised feature selection methods,” *Artificial Intelligence Review*, vol. 53, no. 2, pp. 907–948, Jan. 2020.
- [42] M. Li, T. Zhang, Y. Chen, and A. J. Smola, “Efficient mini-batch training for stochastic optimization,” in *Proceedings of the 20th ACM SIGKDD International Conference on Knowledge Discovery and Data Mining*, New York, USA, 2014, pp. 661–670.
- [43] P. Branco, L. Torgo, and R. P. Ribeiro, “A survey of predictive modelling on imbalanced domains,” *ACM Computing Surveys (CSUR)*, vol. 49, no. 2, pp. 1–50, Mar. 2016.
- [44] S. M. Kasongo and Y. Sun, “A deep learning method with wrapper-based feature extraction for wireless intrusion detection system,” *Computers & Security*, vol. 92, p. 101752, May. 2020.
- [45] A. Tharwat, T. Gaber, A. Ibrahim, and A. E. Hassanien, “Linear discriminant analysis: A detailed tutorial,” *AI Communications*, vol. 30, no. 2, pp. 169–190, May 2017.
- [46] F. Pedregosa, G. Varoquaux, A. Gramfort, V. Michel, B. Thirion, O. Grisel, M. Blondel, P. Prettenhofer, R. Weiss, V. Dubourg, J. Vanderplas, A. Passos, D. Cournapeau, M. Brucher, M. Perrot, and E. Duchesnay, “Scikit-learn: Machine learning in Python,” *Journal of Machine Learning Research*, vol. 12, pp. 2825–2830, 2011.
- [47] P. V. Dinh, D. N. Nguyen, D. T. Hoang, N. Q. Uy, S. P. Bao, and E. Dutkiewicz, “Balanced twin auto-encoder for iot intrusion detection,” in *GLOBECOM 2022 - 2022 IEEE Global Communications Conference*, Rio de Janeiro, Brazil, 2022, pp. 3387–3392.
- [48] P. V. Dinh, N. Quang Uy, D. N. Nguyen, D. Thai Hoang, S. P. Bao, and E. Dutkiewicz, “Twin variational auto-encoder for representation learning in iot intrusion detection,” in *2022 IEEE Wireless Communications and Networking Conference (WCNC)*, Austin, TX, USA, 2022, pp. 848–853.
- [49] K. DP and J. Ba, “Adam: A method for stochastic optimization,” in *Proc. of the 3rd International Conference for Learning Representations (ICLR)*, San Diego, California, US, 2015, pp. 1–15.
- [50] X. Glorot and Y. Bengio, “Understanding the difficulty of training deep feedforward neural networks,” in *Proceedings of the Thirteenth International Conference on Artificial Intelligence and Statistics*, Chia Laguna Resort, Sardinia, Italy, 2010, pp. 249–256.
- [51] J. Chen, S. Sathe, C. Aggarwal, and D. Turaga, “Outlier detection with autoencoder ensembles,” in *Proceedings of the 2017 SIAM International Conference on Data Mining*, Houston, Texas, USA, 2017, pp. 90–98.
- [52] T. Pang, F. Nie, J. Han, and X. Li, “Efficient feature selection via $ell_{2,0}$ -norm constrained sparse regression,” *IEEE Transactions on Knowledge and Data Engineering*, vol. 31, no. 5, pp. 880–893, May 2018.
- [53] J. Snoek, H. Larochelle, and R. P. Adams, “Practical bayesian optimization of machine learning algorithms,” in *Advances in Neural Information Processing Systems*, vol. 25, Lake Tahoe, Nevada, USA, 2012, pp. 2951–2959.